Molecular links between whitesand ecosystems and blackwater formation in the Rio Negro watershed

C. Simon [a,b], T.P. Pimentel [c], M.T.F. Monteiro [c], L.A. Candido [c], D. Gastmans [d], H. Geilmann [e], R. da Costa Oliveira [c], J.B. Rocha [c], E. Pires [c], C.A. Quesada [c], B.R. Forsberg [c,f], S.J.F. Ferreira [c], H.B. da Cunha [c], G. Gleixner [a,*]

[a] *Molecular Biogeochemistry, Max Planck Institute for Biogeochemistry (MPI-BGC), Hans Knöll-Str. 10, 07745 Jena, Germany*
[b] *Institute of Biogeochemistry and Pollutant Dynamics (IBP), ETH Zürich, Universitätstrasse 16, 8092 Zürich, Switzerland*
[c] *Coordenação de Dinâmica Ambiental (CODAM), Instituto Nacional de Pesquisas da Amazônia (INPA), Av. Efigênio Sales 2239, Aleixo, Manaus, Brazil*
[d] *São Paulo State University (UNESP), Centro de Estudos Ambientais, Av. 24A, 1515, Bela Vista, Rio Claro, São Paulo, Brazil*
[e] *Stable Isotope Laboratory (BGC-IsoLab), Max Planck Institute for Biogeochemistry, Hans Knöll-Str. 10, 07745 Jena, Germany*
[f] *Vermont Agricultural and Environmental Laboratory, 163 Admin Dr, Randoph Center, 05602 Vermont, United States*

Abstract

Tropical rivers such as the Rio Negro constitute a major portion of the global aquatic flux of dissolved organic carbon (DOC) entering the ocean, but the exact amount, source contributions and fate of terrestrial DOC remain unknown. We investigated the role of valley and upland whitesand ecosystems (WSEs) and *terra firme* plateaus in forming blackwater tributaries in the Rio Negro basin to develop novel constraints for the terrestrial export of carbon. 5709 molecular markers from ground- and surface waters of two contrasting valley and upland sites feeding Rio Negro tributaries were identified by ultra-high resolution mass spectrometry (FT-MS), analyzed by multivariate statistics and compared to known Rio Negro markers. In a Principal Coordinates Analysis, valley and upland DOC molecular composition differed by 78% from plateau DOC, which was characterized by reworked, aliphatic and unsaturated N- and S-containing molecules, while valley and upland DOC contained mainly condensed aromatics, aromatics and oxidized unsaturated structures. Valley and upland samples differed by 10% in molecular DOC composition and by their isotopic content (^{14}C of SPE-DOC, ^{18}O and ^{2}H of water) which indicated differences in hydrology and C turnover. Against expectation, markers of widespread whitesand valleys did not emerge as a major source of Rio Negro markers, but specific upland markers did. Pubchem suggested chromene and benzofuran structures as promising candidates for further study. Our findings indicate that the export of molecular markers diverges from expected transport-limited DOC behavior, and thereby opens new avenues for source annotation beyond DOC quantity. Terrestrial DOC from upland whitesand areas is a major source of specific blackwater molecules missing in the regional ecosystem C balance, whereas C export from the whitesand valleys and especially from *terra firme* plateaus represents mainly recycled and transformed carbon not directly affecting the ecosystem C balance and possibly, the watersheds downstream molecular signature. Our study highlights the potential of high-resolution techniques to constrain carbon balances of ecosystems and landscapes by novel molecular markers. A comparison with other terrestrial DOM datasets indicated molecular similarities with temperate acidic soils and tropical rivers that warrant further analysis of common DOM markers. Implications,

---

limitations, and future challenges are discussed in the light of potential applications of diagnostic molecular links for DOC source annotation and estimation of terrestrial DOM export in the land-to-ocean continuum.

1. INTRODUCTION

The riverine export of terrestrial dissolved organic carbon (DOC) constitutes a major flux within the boundless carbon cycle that connects land and ocean (Regnier et al., 2013; Drake et al., 2018b; Webb et al., 2018). Global estimates indicate a total of 208 ± 28 Tg DOC exported by rivers each year (Dai et al., 2012), mainly coming from large tropical and circumboreal watersheds (Raymond and Spencer, 2014; Li et al., 2019). Tropical rivers account for a major portion of the flux, being equivalent to 62–66% of global DOC export (Dai et al., 2012; Huang et al., 2012). Moreover, recent modelling efforts show that tropical annual exports have been rising over the past 65 years, with an increase of 10 Tg C compared to 1960 in case of South America (Li et al., 2019). The three tropical rivers with highest discharge, the Amazon (incl. Tocantins), the Congo and the Orinoco, alone deliver 18% of global riverine DOC (Raymond and Spencer, 2014). Due to within-river DOC transformations, actual export of terrestrial organic carbon is expected to be even higher (Abril et al., 2014; Drake et al., 2018b), and novel markers are needed to quantify the original terrestrial part of the carbon export.

Blackwater river basins stand out as hotspots of DOC release in the tropics (Junk et al., 2011). The Rio Negro basin for example, which covers roughly 10% of the area of the Amazon river basin, accounts for an annual DOC export of 5.2–6.7 Tg C (Coynel et al., 2005; Guinoiseau et al., 2016) equivalent to 17–23% of the Amazon's total DOC export (Raymond and Spencer, 2014). Tropical blackwater rivers such as the Rio Negro are thus pivotal in understanding the global carbon cycle and its response to environmental change (Alvarez-Cobelas et al., 2012; Raymond and Spencer, 2014; Webb et al., 2018).

Qualitative analyses of DOC composition have shown great potential to track processes and source contributions on the watershed scale (Creed et al., 2015; Riedel et al., 2016; Hutchins et al., 2017; Drake et al., 2019; Spencer et al., 2019). Processes such as deforestation (Drake et al., 2019; James et al., 2019), drainage (Moore et al., 2013) or warming (Drake et al., 2018a) all affect the molecular composition or age of leached DOC. Progress in qualitative DOC measures could thus effectively complement global and regional modelling efforts based on quantitative DOC export data (Alvarez-Cobelas et al., 2012; Lv et al., 2019). Traditional targeted approaches aiming at terrestrial source markers – mostly polyphenol-type metabolites, such as lignin monomers or tannins – need further complementary insight due to findings suggesting their fast turnover in soils (Gleixner et al., 2002; Hernes et al., 2007; Marschner et al., 2008) and within the land-to-ocean continuum (Cao et al.,

2018) as well as potential autochthonous sources in marine systems (Powers et al., 2019). This places special interest on unknown transformation products that may not be properly accounted for in targeted studies yet but could lead to novel biomarkers (Waggoner et al., 2015; Waggoner et al., 2017). Only a few authors have addressed the traceability and stability of ecosystem imprints within the aquatic land-to-ocean continuum, and its conditions, in a non-targeted way by means of ultrahigh resolution mass spectrometry to identify novel markers (FT-MS; Roth et al., 2014; Medeiros et al., 2016; Hutchins et al., 2017; Wagner et al., 2019). This gap is due to the limited availability of these molecular-level analytical tools. FT-MS techniques allow unprecedented molecular insight by resolving thousands of signals within a single DOM sample, which are assigned molecular formulae based on exact mass (Hertkorn et al., 2013). FT-MS techniques have now added important detail in character and transformation of ecosystem imprints at all stages of the aquatic continuum (Hutchins et al., 2017; Raeke et al., 2017; Kellerman et al., 2018; Lynch et al., 2019; Roth et al., 2019; Wagner et al., 2019). Dedicated sets of novel, traceable ecosystem markers are however rare and need to be calibrated to complement high-resolution DOC flux data (Roth et al., 2014; Medeiros et al., 2016; Riedel et al., 2016; Cao et al., 2018). Robust sets of molecular markers could promote better understanding of ecosystem-resolved DOM export dynamics and its drivers. This knowledge is pivotal to evaluate and predict the vulnerability and biogeochemical functionality of watersheds under environmental change scenarios (McGuire et al., 2014; Abbott et al., 2018; Bernhardt et al., 2018; Jehn et al., 2020).

As described above, the Rio Negro basin is one of the world's largest DOC emitters in terms of estimated annual flux (6.7 Tg DOC) and yield (9.7 g DOC m-2), making it a classic "blackwater" river (Meyer and Edwards, 1990; Coynel et al., 2005; Dai et al., 2012). Scientists early noted the co-occurrence of tropical whitesand ecosystems (WSEs) and blackwater streams, and hypothesized a link between them (Sioli, 1954; Janzen, 1974; Leenheer, 1980; Ertel et al., 1986; Goulding et al., 1988; Junk et al., 2011). The most characteristic feature of WSEs in these landscapes is their sandy soil, classified as either podzol (2% of Amazon basin area) or arenosol (3%) by the World Reference Base (Quesada et al., 2011). These soils differ largely from the more widespread clayey tropical soils such as ferralsols (32%), acrisols (29%), or plinthosols (9%) that are typically found on plateaus and their slopes (Do Nascimento et al., 2004; Quesada et al., 2011; Lucas et al., 2012). Due to the low water-holding capacity of sand, WSEs are also characterized by specific types of vegetation that differ from highly

diverse terra firme rainforests which are dominated by large trees. In the central Amazon, these are sclerophyllous, shruby and smaller-tree dominated *Caatinga*, *Campina*, and *Campinarana* forests, known for their unique plant secondary metabolites and adapted decomposer communities (Janzen, 1974; Klinge and Medina, 1979; Zanchi et al., 2015; Demarchi et al., 2018; Vasco-Palacios et al., 2018). WSEs occur as local upland depressions on plateaus, as intersected valleys forming large riparian corridors at the foot of plateau slopes, or in low-elevation terrain in the form of wide peneplains (Do Nascimento et al., 2004; Montes et al., 2011). Roughly, upland and riparian valley WSEs are dominant in the lower Rio Negro basin while peneplains are widely distributed in the upper Rio Negro basin (Montes et al., 2011). It is likely that the molecular composition of DOM resolves the different environmental conditions, allowing for proper landscape-based DOC source identification and export calculations.

Previous studies that assessed terrestrial sources of Rio Negro DOM largely supported the older hypotheses that WSEs, and more specifically the widely distributed riparian corridors are responsible for the highest amount of carbon export (Junk, 1993; Remington et al., 2007; Melack and Hess, 2010; Bardy et al., 2011). However, this DOC export is mainly controlled by precipitation amount and flooding events (McClain et al., 1997; Remington et al., 2007; Zanchi et al., 2015). This is in line with the finding that in riparian settings, DOC generally shows transport-limited behavior, meaning that its absolute flux scales with discharge (Musolff et al., 2017; Zarnetske et al., 2018). As a result, water passing through the riparian zone continuously leaches existing reserves of processed organic matter (Ledesma et al., 2015; Laudon and Sponseller, 2018; Tiegs et al., 2019). In line with the older hypothesis, McClain and coworkers reported low annual DOC yields for widespread plateau areas (terra firme – ferralsol; 2 g DOC m-2 yr-1) but large yields for a relatively small *Campina* WSE catchment (40 g DOC m-2 yr-1) in the lower Negro basin, north of Manaus. The authors predicted that a WSE molecular DOM signal would thus be easily detectable in higher order rivers within the Rio Negro catchment (McClain et al., 1997), and later studies conducted in the same region corroborated this hypothesis (Remington et al., 2007; Zanchi et al., 2015). DOM from well-developed podzols reflected best the chemical properties of DOM isolates from local groundwater and nearby rivers, indicating a low degree of decomposition of DOM in well-drained sandy soils with low sorption potential (Remington et al., 2007; Bardy et al., 2011). However, no subsequent markers were identified or tracked in the lower reaches of the stream network to assess their environmental fate or marker potential (Bardy et al., 2011). Such novel markers are however needed to study variations in DOM export and spatiotemporal dynamics in riverine DOM sources within a catchment (Hutchins et al., 2017; Bernhardt et al., 2018; Laudon and Sponseller, 2018).

Recently, watershed-specific molecular DOM signatures of the Rio Negro and other Amazon tributaries (Tapajos, Madeira, Solimões) were reported (Gonsior et al., 2016; Simon et al., 2019) that could serve as potential markers of ecosystem DOC exports due to their largely conservative behavior during mixing (Simon et al., 2019). We here make use of these openly available FT-MS DOM datasets and compare them to groundwater, surface, and soil water DOM obtained by solid phase extraction (SPE) and Orbitrap FT-MS measurements. We hypothesized that the overall large export of DOM from riparian WSEs in the Rio Negro basin would allow for the retrieval of Rio Negro-specific markers as assumed by previous studies (McClain et al., 1997; Remington et al., 2007; Bardy et al., 2011). We therefore compared an upland *Campina* forest, and a riparian valley system dominated by *Campinarana* forest, both typical for WSE-podzol systems within elevated terra firme plateaus north of Manaus. We hypothesized that both WSEs and plateaus would differ in terms of water chemistry and DOC properties, and that the SPE-DOM molecular composition would reflect these differences as well, yielding new sets of unique ecosystem markers. We further hypothesized that riparian valley WSE markers would indicate clear overlap with known Rio Negro markers and could thus serve as complementary proxies of land-derived primary production in the Rio Negro basin.

2. MATERIALS AND METHODS

2.1. Field sites and sampling procedures

Groundwater and stream samples were taken in early November 2017 at the end of the dry season/ onset of the rainy season in two protected forest reserves under the responsibility of the Instituto Nacional de Pesquisas da Amazônia (INPA) in Manaus, Brazil (Fig. 1). Both reserves, the Reserva Biológica do Cuieiras – ZF2 (2° 36′32.67″ S, 60°12′33.48″ W, at 40–110 m above sea level, Supporting Information Figure S1) and the Reserva Biológica de Campina (2°35′30.26″ S, 60°01′48.79″ W, at 93–101 m a.s.l., Supporting Information Figure S2) are located about 60–70 km north of Manaus (Zanchi et al., 2014; Marques et al., 2016). We conducted sampling from 31st October – 2nd of November, and all lab procedures followed within three days. The geological setting, landscape structure, forest composition, and soil characteristics have been described in detail by Zanchi et al. (2014). Reserva Cuieiras covers a transect that spans from typical clayey plateaus and slopes (oxisols, ultisols) to broad swampy valleys (podzols, gleysols) while Reserva Campina is widely covered by characteristic sandy soils (podzols) and shows less relief. Reserva Cuieiras is part of a hundred-fold larger watershed but likely exports less DOC per square meter and year (McClain et al., 1997; Waterloo et al., 2006; Monteiro et al., 2014; Zanchi et al., 2014; Zanchi et al., 2015). More information on size of watersheds, water and carbon fluxes are given in the Supporting Information Text S1.

We sampled the stream and five surrounding piezometers in each of the two whitesand ecosystem (WSE) study sites (Supporting Information Figure S3). These samples will be referred to as "valley" (Reserva Cuieiras; see Monteiro et al., (2014) for more details) and "upland" (Reserva Campina; see McClain et al., (1997) for more details) in the following. Valley and upland samples stem
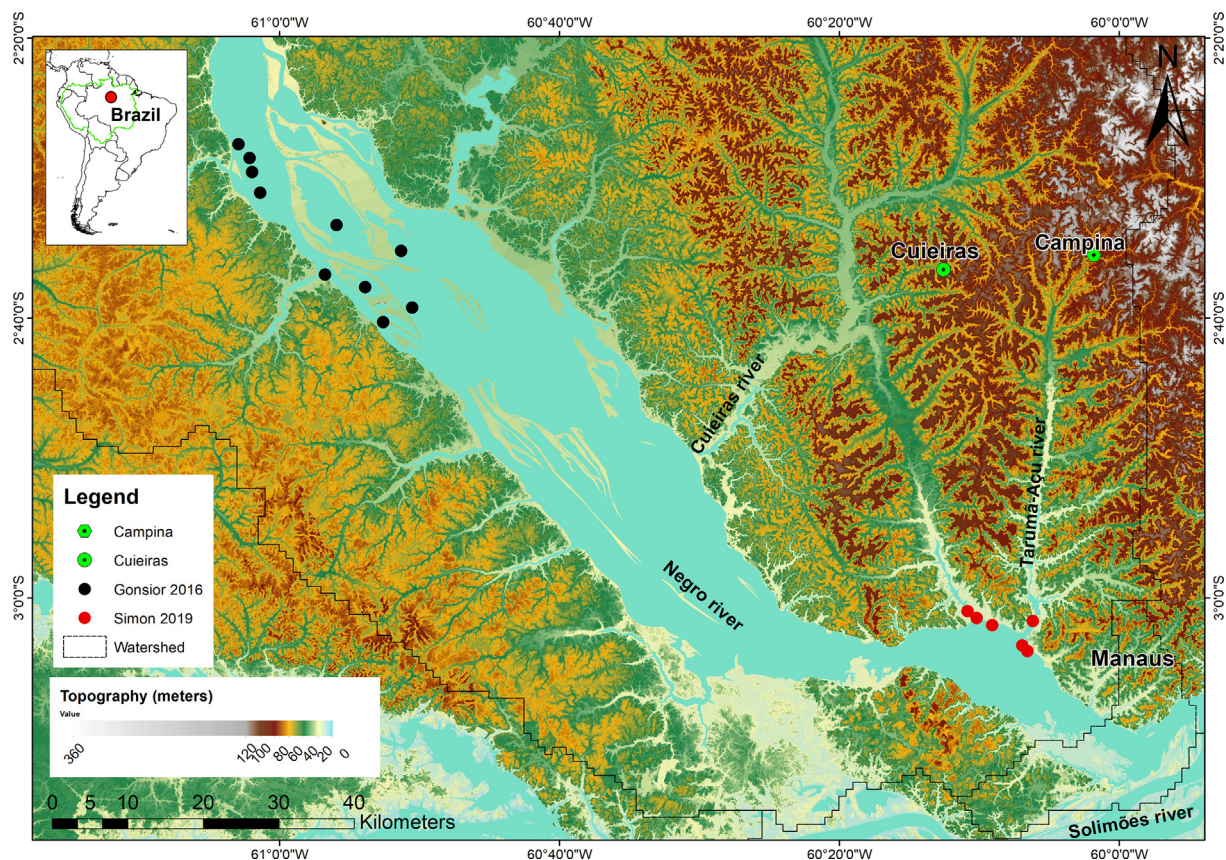
Fig. 1. Topographic detail of the lower Rio Negro catchment northwest of Manaus showing sampling sites of available FT-MS studies (see Supporting Information Figures S1, S2 and S3 for more detail). We sampled groundwater and streams at two headwater locations north of Manaus (green dots; "Cuieiras", "Campina"). Two other FT-MS datasets were used for comparison and are shown as well (black dots, Gonsior et al., 2016; red dots, Simon et al., 2019). Watershed limits and were accessed as shapefiles from www.ore-hybam.org (Seyler et al., 2009). The inset of South America indicates the enlarged section of the map (red dot) and the Amazon basin (green boundary). Map editors: Marcus Guderle, MPI Jena, and Regison da Costa Oliveira, INPA Manaus. (For interpretation of the references to colour in this figure legend, the reader is referred to the web version of this article.)

from low-diversity, low-stature forests characterized by sandy, coarse soils. Both belong to the class of whitesand ecosystems (WSE's, Adeney et al., (2016)) introduced earlier. The valley site is wetter (hydromorphic riparian soils) and more productive (larger trees, *Campinarana* forest) than the upland site which is characterized by smaller trees (*Campina* forest) and overall drier, well-drained conditions (Zanchi et al., 2015).

At Reserva Cuieiras, four additional non-WSE groundwater samples were taken on the *terra firme* plateau (two deep wells) and its adjacent slopes (two piezometers), which will be referred to as a third class of "plateau" samples (for more details see Monteiro et al., (2014)). It is important to realize that the plateau and valley samples stem from the same transect (Reserva Cuieiras) and are thus hydrologically connected. In contrast to WSE's, plateaus (and their slopes) are characterized by high-diversity, productive forests (*terra firme* forests) and clayey, fine-textured soils rich in iron oxides, and thus do not belong to the class of whitesand ecosystems.

We used pre-cleaned (acidified ultrapure water, pH2, HCl, Merck EMSURE®, p.a., ACS grade) Nalgene™

polycarbonate bottles (Fisher Scientific, Schwerte, Germany) for all samples and rinsed each bottle with the respective sample before final sampling. *Piezometers* were emptied one to three times before final sampling. *Streams* were sampled manually, with nitrile gloves, against the direction of flow. *Deep wells* (35 m and 39 m depth) on the plateau were sampled by lowering an empty, clean sampling bottle on a string until water was reached.

2.2. Water chemistry: TOC, pH, electrical conductivity

Aliquots of the samples were subjected to TOC analysis in the water laboratory of the Instituto Nacional de Pesquisas da Amazônia (INPA) in Manaus, Brazil (Laboratório de Águas do INPA/ CPRHC – Coordenação de Pesquisas em Recursos Hídricos e Clima). Samples were measured on a total organic carbon analyzer (TOC-VCPH model, Shimadzu, Kyoto, Japan) (Monteiro et al., 2014). Before extraction, we analyzed samples for pH and electrical conductivity (EC) with a Multi 340i probe system (WTW, Weilheim, Germany).

2.3. Solid-phase extraction of DOM

DOM samples were solid-phase extracted (SPE) shortly after sampling at INPA, Manaus (Laboratório de Ecossistemas Aquáticos) using an established protocol (Dittmar et al., 2008). Samples were acidified to pH 2 with 37% hydrochloric acid (Merck EMSURE®, p.a., ACS grade) before extraction. We used ultrapure water, acidified ultrapure water (pH 2, HCl), and ultrapure methanol (Biotec Reagentes Analíticos, p.a., ACS grade). We loaded columns with maximal amounts of 3 mg C. The extraction efficiency (EE) of samples with high DOC concentrations (>2 mg l-1, n = 11) was always > 60% and on average 71 ± 8%, at a loading ratio of 443 ± 143 (average ± standard deviation; PPL: DOC in mg/ mg; Table 1). Sample PT6 was an exception (high DOC, low EE: 33%). Samples with low DOC concentrations (<2 mg l-1, n = 4) showed lower extraction efficiency (23 ± 15%), and loading ratios were generally higher (2400 ± 960).

2.4. Water isotopes

Isotopic signatures of water (δ^2H- and δ^{18}O-values) were analyzed by high-temperature conversion-isotope ratio mass spectrometry (HTC-IRMS) in the stable isotope laboratory of the Max Planck Institute for Biogeochemistry (BGC-IsoLab). Measurements were conducted on a Delta + XL coupled to a high-temperature furnace (Thermo Fisher Scientific, Bremen, Germany). One µl of water was injected and measured at a furnace temperature of 1350 ° C. For method details, we refer the reader to the literature (Gehre et al., 2004). The δ^2H and δ^{18}O values are reported on the VSMOW scale, which is realized by parallel analysis of samples against in-house standards. In-house standards are routinely calibrated against internationally accepted water standards. Daily standard deviations for δ^2H and δ^{18}O measurements are usually better than 1 and 0.1 ‰, respectively. We accessed regional isotope ratio estimates of rain for October and November with the help of the online isotopes in precipitation calculator (OIPC2.2, version 3.1, http://wateriso.utah.edu/waterisotopes/; Bowen and Revenaugh, 2003). The values were similar for both sites; −7 ‰ and −17 ‰ (V-SMOW) for δ^2H, and −2.4‰ and −3.8‰ (V-SMOW) for δ^{18}O in October and November, respectively. We estimated the average between both monthly values for each isotope, considering our sampling date at the end of October/ beginning of November.

2.5. Radiocarbon analysis of solid-phase extracted DOC (SPE-DOC)

We transferred an aliquot of methanolic PPL extract equivalent to 0.25 mg C to tin capsules (8 mm diameter, 20 mm height; IVA Analysentechnik, Meerbusch, Germany). The methanol was left to evaporate. Air-dried capsules were combusted in an elemental analyzer and graphitized for radiocarbon analysis on a 3 MV Tandetron 14C-AMS (HVEE, Amersfoort, Netherlands) at the Max Planck Institute for Biogeochemistry in Jena, Germany. Modern (Oxalic Acid II) and ^{14}C-depleted standard

Table 1
Combined data of samples described in this study. All samples were taken in 2017. Symbols are explained beneath the table. Abbreviations: EC, electrical conductivity; F^{14}C, Fraction Modern; Δ^{14}C, correction accounting for decay between sample collection and measurement; EE, extraction efficiency based on DOC of samples and SPE extracts.

ID	Group	Specifier	Date	Type	Depth* [m]	pH	EC [µS/cm]	DOC [mg/L]	δ^2H [‰]	δ^{18}O [‰]	d-excess [‰]##	F^{14}C	Δ^{14}C [‰]	Cal. Age [years]	EE [%]
PR11	Plateau	-	11/01	Piez.	0.96*	4.2	14	0.89	−26.8	−5.03	13.44	n.d.**	-	-	6
PR10	Valley	Intermediate	10/31	Piez.	n.d.	4.2	16	2.31	−24.2	−4.50	11.8	0.974#	−33.6#	(2026)#	63
PR9	Valley	Upland-like	10/31	Piez.	0.24*	3.6	54	37.0	−20.2	−3.96	11.48	1.055	46.8	2009	71
PR8	Valley	Upland-like	10/31	Piez.	0.15*	3.6	50	34.1	−16.6	−3.61	12.28	1.056	47.0	2009	80
PR7	Valley	Upland-like	10/31	Piez.	1.12*	3.6	50	37.5	−29.8	−5.11	11.08	1.055	46.1	2009	72
PT6	Valley	Intermediate	10/31	Piez.	n.d.	3.9	29	31.3	−26.4	−4.61	10.48	1.021	12.3	2016	33
PR6	Plateau	-	11/01	Piez.	1.86*	4.5	11	1.80	−24.6	−4.84	14.12	n.d.**	-	-	22
PP1	Plateau	-	11/01	Well	39.0	4.5	12	0.54	−26.6	−4.96	13.08	n.d.**	-	-	42
PP2	Plateau	-	11/01	Well	35.0	4.7	10	0.56	−28.9	−4.86	9.98	n.d.**	-	-	20
RA	Valley	Intermediate	10/31	River	0	4.3	14	6.29	−23.3	−4.44	12.22	1.035	26.4	2013	80
P2	Upland	-	11/02	Piez.	2.4	3.6	55	36.9	−7.2	−2.75	14.8	1.063	53.8	2008	60
P4	Upland	-	11/02	Piez.	1.5	3.9	40	28.2	−18.2	−3.77	11.96	1.055	46.4	2009	72
P5	Upland	-	11/02	Piez.	1.5	3.8	43	30.4	−15.9	−3.69	13.62	1.072	63.6	2006	73
P6	Upland	-	11/02	Piez.	1.5	3.6	50	45.7	−15.9	−3.67	13.46	1.079	70.5	2004	63
P7	Upland	-	11/02	Piez.	1.5	3.6	52	38.5	−17.6	−3.77	12.56	1.074	64.7	2005	79
RC	Upland	-	11/02	River	0	3.6	54	46.4	−16.4	−3.79	13.92	1.070	61.7	2006	62

* Plateau and valley samples: In piezometers, water level below the surface at sampling (daily mean, hourly data), in wells: maximum depth. In upland samples: piezometers, max. depth. ** n.d., not determined due to the limited amount of extract. # Value likely influenced by ^{14}C-dead contaminant signal. ## Calculated based on the formula d-excess = δ^2H – 8* δ^{18}O (Dansgaard, 1964).

materials were carried along for quality control and data corrections (Steinhof et al., 2017; Benk et al., 2018). Graphitization is conducted with Duran glass tubes at a temperature of 550 °C in the presence of hydrogen and with an iron catalyst (Steinhof et al., 2017). Radiocarbon concentrations are given as fraction modern ($F^{14}C$), which is the fraction of the standard concentration normalized for $\delta^{13}C$ of the oxalic acid standard measured at the same time (with $\delta^{13}C$ of $-19‰$; Trumbore et al., 2016). $\Delta^{14}C$ values also take into account radioactive decay of the oxalic acid standard since 1950, which demarks the start of bomb tests that increased the ^{14}C content of the atmosphere (Trumbore et al., 2016). We calibrated our background-corrected $F^{14}C$ data with atmospheric data published in Graven (2015) to derive SPE-DOC age. We used values for the inter-tropical convergence zone (zone SH3). To cover the timepoint of sampling (2017), we predicted $\Delta^{14}C$ values for 2016 and 2017 based on data from 1997-2015 by linear regression ($R2 = 0.996$) and then estimated SPE-DOC mean calendar age. The measurement error was < 1 year and < 2 years for repeated measurements (standard deviation).

2.6. Orbitrap measurements of SPE-DOM and data processing

We conducted Orbitrap measurements at the Max Planck Institute for Biogeochemistry, as described elsewhere (Simon et al., 2018), at a nominal resolution setting of 480.000. Data processing and formula assignment followed similar rules as given in Simon et al. (2019) and are specified in Supporting Information Text S2. In short, after raw data processing, 13658 peaks remained in the dataset in total. Allowable numbers of atoms in formula calculations were as follows: ^{12}C, 0–60; ^{1}H, 0–120; ^{14}N, 0–2; ^{32}S, 0–1; ^{16}O, 1–60, ^{13}C, 0–1, and the assignment was done at $\pm$ 1 ppm tolerance. After further application of common rules for exclusion of false positives (Herzsprung et al., 2014; Riedel and Dittmar, 2014; Hawkes et al., 2016), the final dataset contained 7705 formulae (of those, 1963 containing a ^{13}C; Supporting Information Text S2). For comparison of samples, we normalized all mass spectra to the sum of their peak intensities (including all peaks > S/N = 5, also those with no assigned formula). The further analysis of the data focused on the subset of peaks with an assigned monoisotopic formula (n = 5709). The crosstab is available from https://doi.org/10.1594/PANGAEA.922606 (Supporting Information Data Set S1, "ds01").

2.7. Statistical analyses: Significant differences, ecosystem fingerprints and molecular links

We tested the environmental data and SPE-DOM trends for significant differences between groups of samples. We checked the data for normality, variance homogeneity and normality of residuals with established tests before running ANOVA or Kruskal-Wallis tests followed by post hoc tests in the statistical computation environment R Studio (see details in Supporting Information Table S1, v1.2.5019, © 2009–2019 RStudio, Inc.). We also analyzed

the molecular formula data in RStudio by Principal Coordinate Analysis (PCoA, cmdscale function, stats package, v3.5.1) and post-ordination gradient fitting analysis (envfit function, vegan package, v2.5–2). PCoA was based on Bray-Curtis dissimilarities obtained by the function vegdist from package vegan (Oksanen, 2010) and is described in detail elsewhere (Osterholz et al., 2016). We additionally analyzed the PCoA distribution of samples for clustering (indicating similarity among samples) and correlations with specific DOM indices by the envfit function (at 999 permutations). DOM indices aggregate properties of the molecular formula population of each sample (Supporting Information Table S2). We finally assessed molecular formulae with a significant (p = 0.05) association to clusters of samples derived from PCoA analyses by Student's t-test of averaged relative ion abundances across samples of each group. We conducted two-sided tests assuming unequal variances to separate "*unique*" from shared but non-informative ("*common*") markers.

To link headwaters and downstream signals, we compared sets of specific molecular formulae to known Rio Negro-specific markers available from two open-access FT-MS datasets (Gonsior et al., 2016; Simon et al., 2019). These datasets and details of our Rio Negro marker definitions are described in Supporting Information Text S3. In short, we extracted the robust markers of Rio Negro by using most abundant and unique DOM molecular formulae as assessed by large-scale differences among Amazon tributaries (Gonsior et al., 2016) or by using DOM formulae that were correlated with the amount of Rio Negro water in repeated mixing experiments with the mainstem Rio Solimões (Simon et al., 2019). The majority of the indicative Rio Negro markers were formulae containing only C, H and O atoms (CHO formulae). The three datasets were also merged to allow an analysis of general comparability of published SPE-DOM data from the Rio Negro basin (analysis presented in Supporting Information Text S3). The merged data from all three studies is available in presence/absence format and with ion abundance information from https://doi.org/10.1594/PANGAEA.922606 (Supporting Information Data Set S2, "ds02"). We queried PubChem for a subset of these markers. Twelve ions, one hydrate and six stereoisomers were excluded from the list of structural suggestions (Supporting Information Data Sets S1 and S3, "ds01" and "ds03").

3. RESULTS

3.1. Water chemistry and isotopic composition of water and SPE-DOC

Samples were clearly differentiated by water chemistry. Acidity (pH), electrical conductivity (EC) and concentrations of dissolved organic carbon (DOC) were 3.7 ± 0.1, 49 ± 6 µS cm^{-1} and 37.7 ± 7.54 mg C l^{-1} across all upland samples (Fig. 2a – c, Table 1), and some of the valley samples (PR7, PR8, PR9, Table 1) indicated the same tendency. The four plateau samples showed slightly higher pH, and low EC and DOC levels (4.5 ± 0.2, 12 ± 2 µS cm^{-1} and 0.9 ± 0.6 mg C l^{-1}). In contrast to the upland samples,
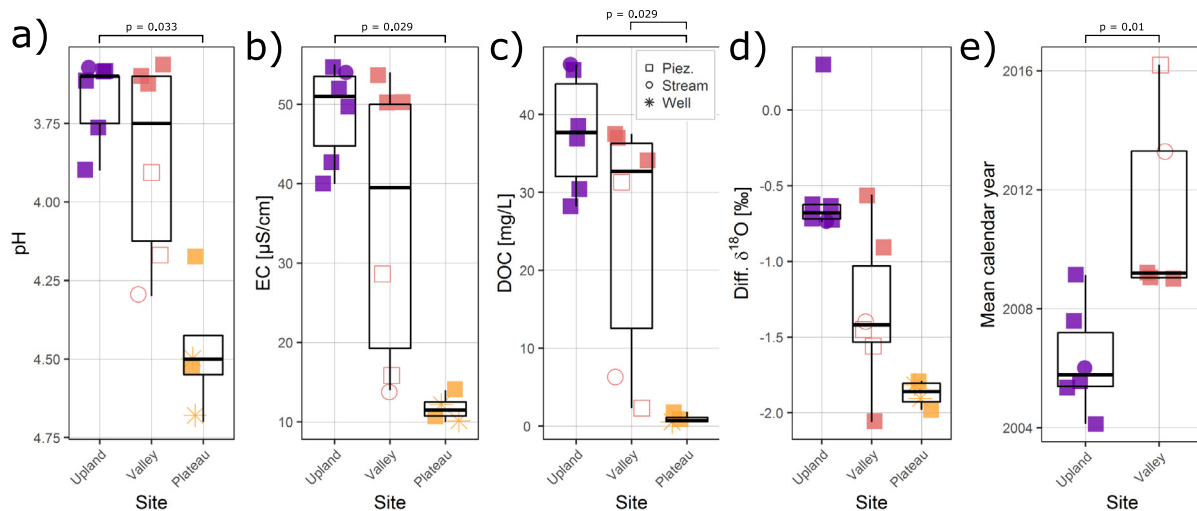
Fig. 2. Differences in the water and SPE-DOC properties. Variables shown are a) pH, b) electrical conductivity, c) dissolved organic carbon concentration, d) difference in $\delta^{18}O$ values of water compared to regional average precipitation (OIPC estimate), e) mean calendar age of DOC in solid-phase extracts. Samples are grouped into biogeochemical environments (upland; valley, and plateau, see Supporting Information Figure S3 for locations). Symbols denote sample type (squares, piezometer; star, deep well; circle, stream); open symbols mark "intermediate" valley samples (see main text). Significant differences between groups are denoted on top of each plot with p-level (see Supporting Information Table S1). Non-significant differences (p > 0.05) were omitted.

water chemistry of the valley stream (RA) and two piezometers (PT6, PR10) indicated lower (DOC, EC) or higher values (pH) than those of other surrounding piezometers (Fig. 2, open symbols).

Despite similarities in water chemistry of valley and upland samples (Fig. 2a-c), they differed in water isotopic composition and radiocarbon content of SPE-DOC (Table 1, Fig. 2d-e, Supporting Information Figure S4, Supporting Information Figure S5). All samples plotted on the local meteoric water line, resembling the range of expected isotopic composition found in the region. However, water was overall lighter as compared to local precipitation in previous years (Supporting Information Figure S4). Trends in δ^2H and $\delta^{18}O$ were similar, so we always refer to both isotopes in the following ("water isotopic composition"). Plateau samples showed consistently lighter (more negative) δ^2H and $\delta^{18}O$ values as compared to upland samples. In line with larger variation of DOC, EC, and pH, water isotopic composition showed high variation in the valley samples. In contrast, the $\delta^{13}C$ composition of SPE-DOC was very similar across WSE samples (average ± standard deviation: −29.40 ± 0.45 ‰, n = 11) and calibrated radiocarbon ages were very young (less than 2 to 13 years old at maximum). However, upland samples were characterized by a slightly older SPE-DOC (Fig. 2e). Valley and upland streams showed similar water and SPE-DOC isotopic composition as the surrounding piezometers.

3.2. SPE-DOM characterization by ultrahigh-resolution mass spectrometry

The analysis of SPE-DOM molecular composition reflected the separation of samples based on water and

SPE-DOC properties presented above (Fig. 2). The PCoA separated samples into two main clusters (plateau vs. valley/ upland) on the first coordinate, holding 78% of variation (Fig. 3a). Consequently, PCoA 1 was linked to significant (Pearson' r, p < 0.05) trends in pH, EC, and DOC (Fig. 2). The explained variability of PCoA 2 was smaller (10%) but valley and upland samples were clearly separated and thus linked to differences in water isotopic composition and SPE-DOC radiocarbon age (Fig. 3a). PCoA also indicated convergence of differing trajectories of SPE-DOM processing in upland and valley settings. Stream samples showed similar SPE-DOM composition as surrounding piezometers in both settings. Molecular indices derived from the SPE-DOM data were significantly correlated to separation of the plateau, valley and upland clusters (Fig. 3b, c; definitions of indices, see Supporting Information Table S2; tests, see Supporting Information Table S1 and Figure S6). SPE-DOM from valley and upland sites had higher proportions of aromatic and highly oxidized molecular formulae while plateau SPE-DOM was less oxidized and dominated by aliphatic N- and S-containing formulae (Fig. 3b, c). Low numbers of N-containing formulae and a higher average molecular weight differentiated upland from valley SPE-DOM on PCoA 2.

Molecular formulae that separated upland, valley and plateau samples (Fig. 3a) were extracted from the data to obtain individual ecosystem markers or "fingerprints" (Fig. 4, Supporting Information Figure S7, and Supporting Information Figure S8). It is important to note that our definition of "unique" and "common" relates to significant differences in ion abundance. In fact, most molecular formulae were shared based only on presence (30% shared among all three ecosystems, and 83% among valley and upland; Supporting Information Figures S9 and S10).
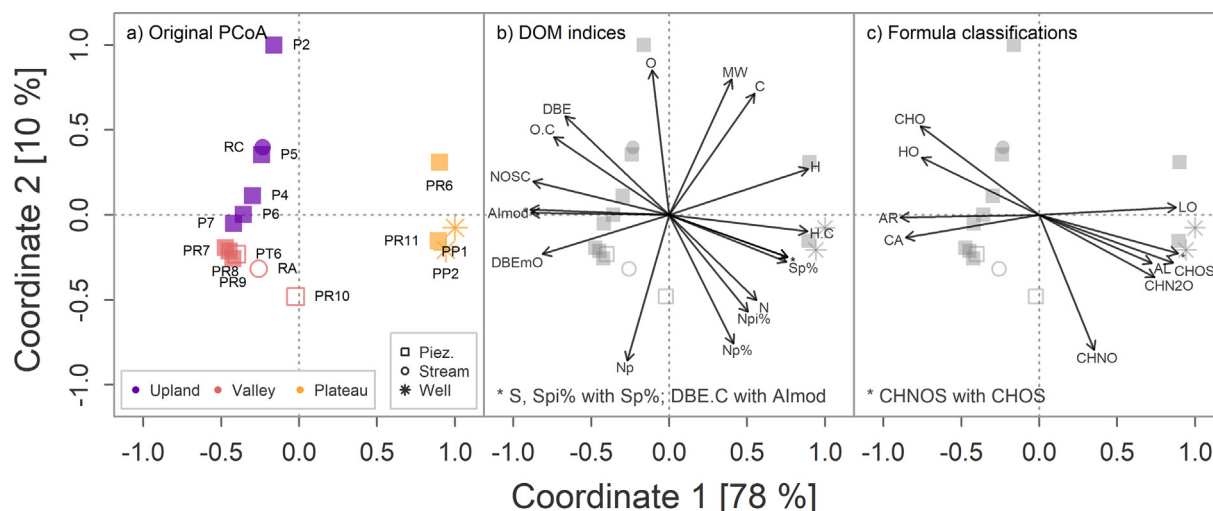
Fig. 3. Multivariate analysis based on molecular SPE-DOM data. a) Separation of samples in a principal coordinate analysis (PCoA) based on Bray Curtis dissimilarity. The plot shows only the first two coordinates, the third coordinate (5% of explained variability, not shown) did not contribute further to separation. Percentages denote the degree of explained variability in SPE-DOM molecular composition. Samples are grouped into biogeochemical environments ("upland", "valley", "plateau"). Symbols denote sample type (square, piezometer; star, deep well; circle, stream); open symbols mark "intermediate" valley samples (see main text). b, c) Post-ordination gradient fit (function envfit of R package vegan, at 999 permutations) of three different sets of variables based on PCoA separation (same as in a). Variables sets are b) SPE-DOM indices, c) Molecular groups, and d) Formula classes. Significant correlations (Pearson, $p < 0.05$) with the ordination are shown as arrows. Arrow length corresponds to the strength of correlation and arrows head into the direction of the steepest increase of the respective variable, based on the ordination pattern of samples. Variable abbreviations in b): C, H, O, N, S (average numbers of respective atoms per formula), MW (molecular weight as mass to charge-ratio), AImod (Aromaticity index), DBE, DBEmO, DBE.C (double bond equivalents, DBE minus oxygen, DBE/C ratio), H/C (atomic ratio of hydrogen to oxygen, "saturation axis"), O/C (atomic ratio of oxygen to carbon, "oxidation axis"), NOSC (nominal oxidation state of carbons), Np, Np%, Npi% (number, percentage and relative abundance of N-containing peaks), Sp, Sp%, Spi% (same for S-containing peaks). Abbreviations in c): CA, condensed aromatics, AR (aromatics), HO (high O unsaturated), LO (low O unsaturated), AL (aliphatics), CHO (average number of molecular formulae containing only C, H and O atoms), CHNO, CHN2O, CHOS, CHNOS (formulae containing one N, two N atoms, one S atom, or both one N and S atom).

Plateau SPE-DOM markers showed a narrow m/z and chemical space distribution (Fig. 4b, c; markers on average centered at 413 ± 13 Da, O/C 0.38 ± 0.01, and H/C 1.27 ± 0.01). 63% of all plateau markers were N- and S-containing formulae (Fig. 4a-c, and Supporting Information Figure S8a), and 81% were classified as unsaturated and less oxidized ("LO"; average NOSC, -0.48 ± 0.02). In contrast, CHO formulae represented 70% of molecular markers common to WSE samples and showed a broad molecular weight range (centered at m/z 344 ± 24 Da, range m/z 150 – 800; Supporting Information Figure S8a-c). On average, > 85% of these formulae were classified as condensed aromatics ("CA", 25%), aromatics ("AR", 35%) or highly oxidized, unsaturated compounds ("HO", 26%; Supporting Information Figure S8b, c).

Valley and upland samples were separated by a sharp "cutoff" at ~ m/z 400 (Fig. 4d, g). 56% of all valley markers were lower-molecular-weight N-containing formulae (on average, m/z 290 ± 6 Da; Supporting Information Figure S8b) classified as condensed aromatics ("CA", 34%) aromatics ("AR", 31%) or oxidized, unsaturated compounds ("HO", 20%). Upland markers were classified similarly (CA, 22%; AR, 44%; HO, 17%), but more formulae were indicative (on average per sample, 1146 vs. 852), thus explaining the higher aromaticity (AImod, 0.55 ± 0.02 vs. 0.48 ± 0.03). 80% of upland markers were simple oxidized formulae (CHO) with higher average mass (391 ± 24 Da)

and a relatively high oxidation state (O/C, 0.57 ± 0.01 vs. 0.37 ± 0.01; NOSC, 0.37 ± 0.03 vs. -0.18 ± 0.03).

3.3. Molecular links between terrestrial ecosystems and the aquatic continuum

We compared the sets of distinct SPE-DOM markers of the valley and upland samples to known Rio Negro markers (Fig. 5). Indicative Rio Negro markers were almost exclusively oxidized, aromatic compounds (CHO formulae; molecular groups "CA", "AR", "HO"). A general comparison of the three datasets used for this analysis is given in the Supporting Information (Supporting Information Text S3, Figures S11 and S12). A cluster of heavy, highly oxidized, and aromatic upland markers indicated consistent overlap ("matching") with Rio Negro markers (Fig. 5). Upland markers (40% and 51% to Simon et al., 2019; Gonsior et al., 2016, respectively) and markers common to the upland and valley samples ("WSEcom", 33% and 26%) showed highest degree of overlap and appeared in a confined area of the Van Krevelen plot (boxes in Fig. 5b, d; ranges: H/C 0.4 – 0.8, O/C 0.4 – 0.8). Valley markers and plateau markers showed less overlap (<7% and < 2%). Overlap in Rio Negro and upland markers was linked to different sets of Rio Negro markers, as indicated by their higher (m/z 350 – 650, Fig. 5c) or lower mass range (m/z 200 – 500, Fig. 5f). Only thirteen formulae were
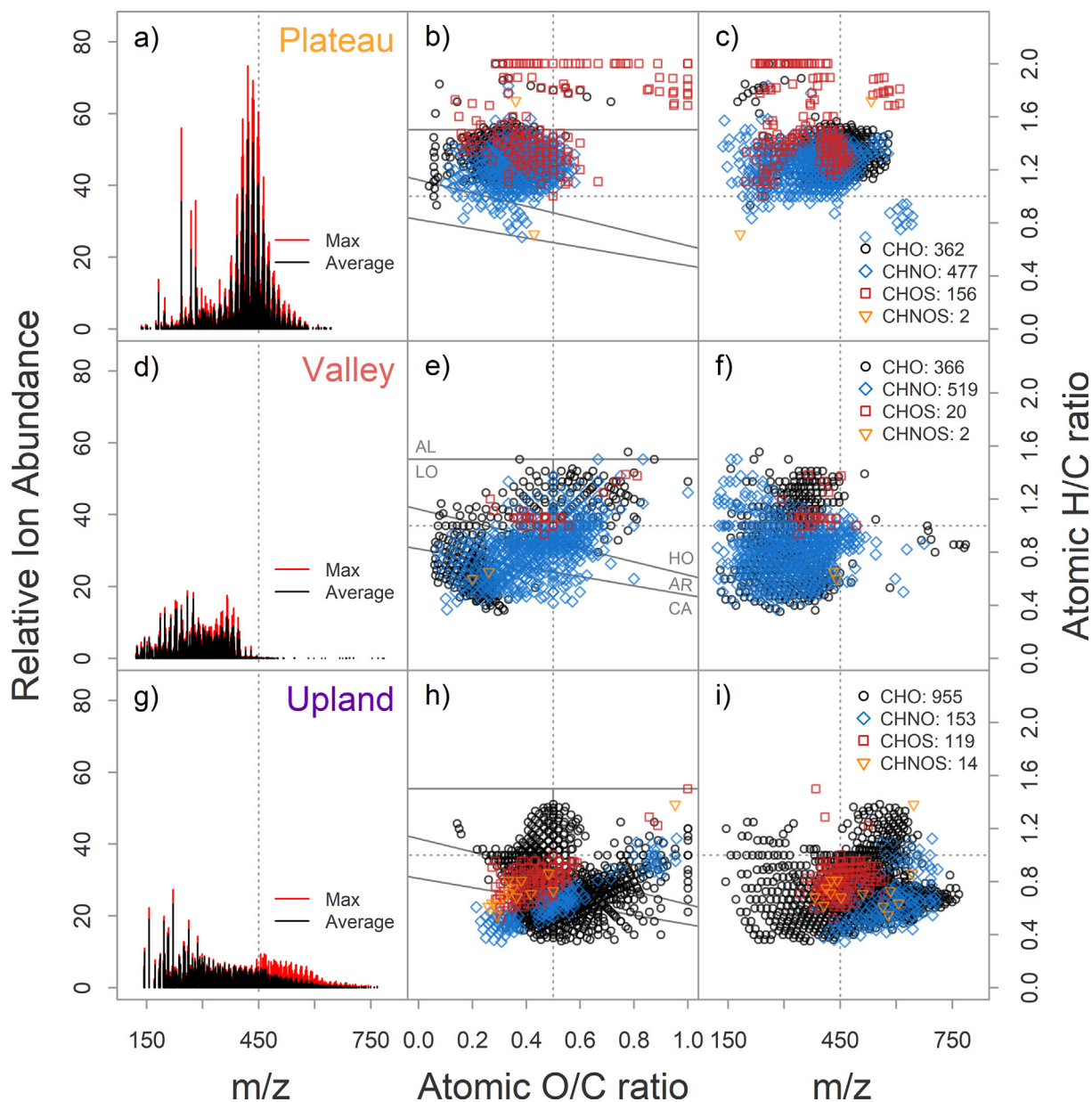
Fig. 4. Molecular fingerprints of ecosystems. Subsets of molecular formulae showing significant "enrichment" (higher ion abundance), i.e., ecosystem specificity, in the plateau (panels a-c), valley WSE (d-f) and upland WSE samples (g-i). General WSE (valley and upland) markers and non-significant signals (common to all samples) are shown in Supporting Information Figure S7. Left column panels (a, d, g) show the average (and max) mass spectrum of each ecosystem. Mid column panels (b, e, h) show the formula subsets in chemical space (Van Krevelen plot, each dot represents a molecular formula defined by its atomic ratios of hydrogen, H/C, and oxygen to carbon, O/C. Formulae are colored according to classes (see legend and numbers of formulae in panels to the right). The plot is divided by solid lines that mark molecular group categories (see also caption of Fig. 3). Right column panels (c, f, i) show the same formula subsets from mid-row panels in H/C vs. m/z (mass-to-charge) space. Dotted grey lines are for visual guidance and comparison (at m/z = 450, O/C = 0.5, and H/C = 1). Left- and right-column plots share the m/z abscissa (x-axis) while mid- and right-column plots share the H/C ordinate (y-axis).

members of both Rio Negro marker sets. Nine of those were also indicative upland markers (six specific to upland, three to both valley and upland; "Upland overlap", red squares in Fig. 5). Pubchem yielded 5 to 108 structural for these nine markers (for formulae $C_{11}H_6O_8$ and $C_{10}H_6O_6$, respectively). Suggested structures were highly oxidized, showing on average 2.5 carbonyl groups, 0.97 ether bonds, and 0.65 lactone groups per molecule. All

formulae were classified as aromatics ("CA", "AR"). On average, 68% of suggested structures per formula had at least one heterocyclic ring (each 30% of five and six-membered rings on average). Functional group count was strongly correlated with mass ($R^2 = 0.84$, range = 5.2 – 9.7), same as numbers of carbon double bonds (0.86, 3.2 – 8.4) and aromatic rings per molecule (0.87, 0.6 – 2.6). Suggestions of smaller molecules (<300 Da, with
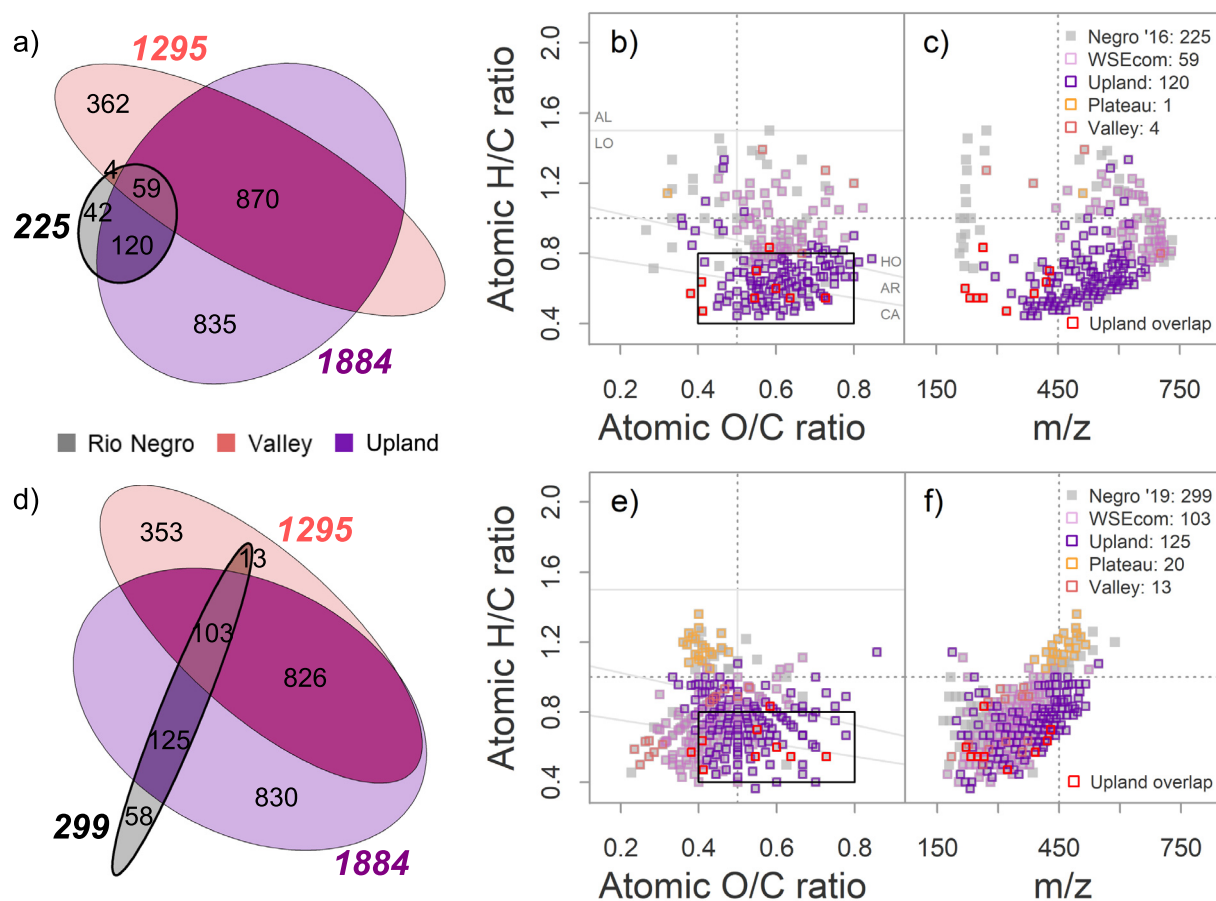
Fig. 5. Analysis of molecular links between headwater ecosystems and Rio Negro markers. Overlap of WSE-specific formulae (significantly enriched formulae) with two independent sets of Rio Negro SPE-DOM markers (a-c: data from Gonsior et al., 2016; d-f: data from Simon et al., 2019). Left panels (a, d) show the overlap of three sets of markers (Rio Negro, valley, upland) in a Venn diagram created with package "eulerr" in RStudio. Overlap indicates common formulae, i.e., shared information. Areas are scaled to number of formulae, which are given for each subset (note color, area may be dissected). Overlap is shown only for CHO formulae because Rio Negro markers were mainly CHO-type, other formula classes showed no distinct overlap. Right panels show Rio Negro markers of each study (grey filled squares) in chemical space (b, e) or H/C vs. m/z plot (c, f; similar visualization as in Fig. 4). Colored symbols show the match between datasets ("overlap") and refer to the bold ellipse in panels a and d, respectively. Plateau markers are additionally added for comparison. Red squares denote the small set of WSE markers that were found to match with both sets of Rio Negro markers. They were uniquely enriched in upland (n = 6) or common to upland and valley WSE's (n = 3). Based on the chemistry of these nine formulae, the black box denotes the wider area of consistent matching in terms of chemical space (H/C 0.4 – 0.8; O/C 0.4 – 0.8). Independent of the underlying set of Rio Negro markers, the matching rate was higher for upland WSE markers (lilac). (For interpretation of the references to colour in this figure legend, the reader is referred to the web version of this article.)

less than 15C atoms) were by tendency naphthalene and chromene structures. Larger molecules > 300 Da (with > 15C atoms) showed more similarities with benzofuran, phenol or benzene-carboxylic moieties.

4. DISCUSSION

4.1. General biogeochemistry of water and carbon

The general analysis of water chemistry revealed two major classes of samples (plateau vs. upland/ valley; Table 1; Fig. 2) which goes along with differences in soil texture and forest types (see section 2.1: Field sites and sampling procedures). Magnitudes and correlations of pH, EC, and DOC concentration agreed with previous reports

(Do Nascimento et al., 2008; Bardy et al., 2011; Monteiro et al., 2014). As plateau samples and valley samples stem from the same study transect (Reserva Cuieiras), some valley samples including the stream were likely plateau-influenced, i.e., affected by mixing due to plateau water supply (Fig. 2, "intermediate" samples). In contrast, the overall homogenous water chemistry of the upland samples indicated less mixing and more direct contact between the stream and its surrounding (McClain et al., 1997; Zanchi et al., 2015).

Local differences in ecohydrology can explain the heavier isotopic composition of groundwater and stream water in the drier upland site (Supporting Information Figure S4; Zanchi et al., 2014; Zanchi et al., 2015), and the lighter isotopic composition of water in the valley, its stream and

the adjacent plateaus (Leopoldo et al., 1982; Kunert et al., 2017): While isotopically heavy samples in upland and valley settings likely reflected a major contribution of recent (dry season) precipitation, groundwater replenished during previous wet seasons explains the lighter water isotopic composition in samples from the plateau and its adjacent slope. This is because water isotopic composition changes predictably between wet and dry seasons and thus can serve as a proxy of water age and source (Leopoldo et al., 1982; Tomasella et al., 2007; Zhang et al., 2009; Miguez-Macho and Fan, 2012; Jasechko and Taylor, 2015; Zanchi et al., 2015; Supporting Information Figure S5).

The $\delta^{13}C$ signature of SPE-DOC reflected a similar C3 vegetation in all samples as reported earlier (Hedges et al., 1986a; Quay et al., 1992). Our data indicate exceptionally fast export of a significant fraction of valley and upland DOC within less than two decades which agrees with lower DOC retention in the characteristic sandy soils of these sites (i.e., regional chromatography model; Hedges et al., 1986b; Hedges et al., 1994; see section 2.1). Young SPE-DO^{14}C ages have been explained by a fast release of fixed C in tropical forests (Hedges et al., 1986b; Mayorga et al., 2005). The slight but consistent differences in radiocarbon age between the drier upland and the wetter valley likely relate to differences in short-term organic matter turnover and accumulation. Productivity, litter turnover and soil respiration rates are lower in upland settings (Zanchi et al., 2011; Zanchi et al., 2014) while DOC export is higher (McClain et al., 1997; Zanchi et al., 2015). In line with these findings, isotopic information showed that sandy tropical environments need to be further distinguished in terms of quality of released DOC.

4.2. SPE-DOM fingerprints reflect differences between clayey and sandy soils

In line with our initial hypothesis, the molecular analysis of SPE-DOM strongly reflected both the major distinction between ecosystem types (plateau vs. valley/ upland samples) and the minor distinction between valley and upland samples (Fig. 3). Markers of plateau and valley/ upland settings (Fig. 4, Supporting Information Figure S7) documented a major soil texture effect on SPE-DOM properties. Fine-textured soil as the one present at plateau sampling sites can cause longer water retention and contact times between minerals, microbes, and water (Marques et al., 2004; Remington et al., 2007) as opposed to the more coarse, sandy soil surrounding valley and upland sampling sites. A finer texture favors lower DOC levels due to intensified decomposition or sorption (Marques et al., 2010). Fine clay and organic particles are also often associated with larger amounts of N-containing compounds (Hedges et al., 1986a; Hedges et al., 1994; Chassé et al., 2015; Newcomb et al., 2017), and newly synthesized, larger and N-containing microbial compounds can become dominant during decomposition (Roth et al., 2019). Molecular characteristics, i.e., aromatic, oxidized, higher molecular weight CHO markers in valley and upland settings, and unsaturated, aliphatic, N-rich SPE-DOC in plateau settings (Fig. 3b, c), were in line with known bulk characteristics

of DOC endmembers from soils and groundwater in the region, for example narrow C/N ratios of DOC (~10) in plateau soils (Leenheer, 1980; McClain et al., 1997; Remington et al., 2007). In turn, valley and upland markers represented initial stages of litter decomposition that agree with reports on wider C/N ratios in whitesand settings (>15, up to 60; McClain et al., 1997). C/N ratios derived from SPE-DOM data showed a remarkable correlation with the DOM data of McClain et al. (1997) (Supporting Information Figure S13). These results demonstrate the overall importance of WSEs for the quality of exported terrestrial DOC in the lower Rio Negro basin, and a good comparability of SPE-DOM with reported DOM data from similar environmental settings. Despite similar trends, C/N estimates based on SPE-DOM also indicated a ~ factor ten bias against N during SPE (Stücheli et al., 2018) or electrospray ionization, which will be discussed further in section 4.5.

4.3. SPE-DOM fingerprints reflect differences between whitesand ecosystems

Distinct differences in SPE-DOM composition between valley and upland samples may be linked to the frequency of drying/ rewetting events (non-saturated/ saturated conditions), which was also suggested by differences in water isotopic composition and SPE-DO^{14}C age. We expected that valley SPE-DOM fingerprints would partly reflect the lateral flows from adjacent plateaus as they were sampled from a transect that is hydrologically connected. The presence of unsaturated N-containing markers supported this hypothesis (compare Fig. 4b, c and e, f). However, distinct markers indicated unique processes in valley and plateau samples. Plateau markers indicated anoxic conditions in older groundwater (lowest NOSC in this study; compare Bhattacharyya et al., 2018). The shift in molecular composition between valley and plateau demonstrates the loss of the plateau SPE-DOM signature of groundwater upon transit through the valley. This finding is remarkable because the riparian zone (i.e., the valley floor) concentrates the water flux that is sourced from the surrounding plateaus (Miguez-Macho and Fan, 2012a) and drives the steady export of young SPE-DOM from the valley, thereby overprinting the plateau SPE-DOM signature (Ledesma et al., 2015). Permanent saturation in the valley, i.e., stagnating waters with depleted oxygen levels, likely contributed to the preservation of reduced organic matter that is partly imported from the surrounding plateaus (Bardy et al., 2011; Boye et al., 2017; Bhattacharyya et al., 2018). Such conditions have been described in riparian settings at the site (presence of specific palm species; Junk, 1993; Luizão et al., 2004) and in the region (elevated levels of NH_4^+ and Fe_2^+, depletion of oxygen; McClain et al., 1994).

Upland SPE-DOM markers, in contrast, represent an "undiluted" signal of initial plant decomposition products of lignin, cellulose, tannin, flavonoids, and terpenoids (Fig. 4g-i). Under non-stagnating, well-drained conditions, sandy soil such as the one present at the upland site favors a quicker escape of such molecules to streams (McClain et al., 1997; Remington et al., 2007), but the older SPE-DO^{14}C age also indicated slightly reduced turnover of these

molecules in upland settings. This is in line with lower rates of litter turnover and CO_2 respiration as noted above (Zanchi et al., 2011; Zanchi et al., 2014). Elongated periods of drought and an adapted plant and decomposer community emerge as main drivers of such ecosystem-level differences. Fungi can remain active under dry and acidic conditions (Rousk et al., 2010; Vasco-Palacios et al., 2018) and may potentially alter DOM towards higher-molecular weight, aromatic, and oxidized structures (Waggoner et al., 2015; Zavarzina et al., 2018), all of which were observed in upland groundwater (piezometer) and stream SPE-DOM. Contributions of pre-aged soil organic matter in upland settings cannot be ruled out at this point and could also explain the mobilization of an apparently older DOC fraction, for example from ongoing podzolizations (Do Nascimento et al., 2008; Bardy et al., 2011).

4.4. Upland whitesand ecosystems are a potential source of indicative Rio Negro markers

We found a clear distinction between potential sources of known sets of Rio Negro markers that could be suitable to quantify terrestrial transfer of organic carbon to the regional aquatic continuum and beyond (Fig. 5). While the matching with plateau markers was negligible, the two whitesand ecosystems (upland and valley) clearly differed in terms of matching markers and indicated – against our initial hypothesis – no major riparian valley but an upland source.

Differences in overlap among both available datasets of Rio Negro markers (Fig. 5b, e; Gonsior et al., 2016; Simon et al., 2019) does not diminish the consistent match in terms of chemical space (black boxes in Fig. 5b, e). Fine-tuning of ion accumulation times, for example, is known to affect ion abundance patterns in FT-MS measurements of DOM (Hawkes et al., 2016; Simon et al., 2018). The comparability of instruments and datasets discussed herein has been addressed recently (Simon et al., 2018; Simon et al., 2019; Hawkes et al., 2020) and is discussed in more detail in the Supporting Information (Supporting Information Text S3, Figures S11 and S12). In short, despite sample set and lab/ instrument effects, measurement settings were relatively similar among the available studies and ours, which suggests that the overlap of upland WSE and Rio Negro markers is no artifact but a sign of robust matching, in line with recent findings from an international FT-MS lab comparison (Hawkes et al., 2020). Thus, while it is not surprising to see large differences in marker sets (given the differences in sampling locations and times, and labs), it is even more remarkable to find consistent overlap between studies, pointing toward subsets of markers with specific oxidation and saturation states. All in all, it is highly encouraging to find consistent and robust molecular overlap in three independent FT-MS datasets, being in line with long-standing hypotheses of landscape functioning in the Rio Negro basin (Leenheer, 1980; Goulding et al., 1988; Hedges et al., 1994), namely that whitesand ecosystems are potential sources of indicative Rio Negro markers.

Counter-intuitively, the highly indicative set of upland markers were not only found to overlap with Rio Negro

samples from the proximity of its draining higher-order river, the Rio Tarumã Açu (Simon et al., 2019) but also in samples upstream (Gonsior et al., 2016; compare Fig. 1). This observation implies that similar upland markers are exported upstream of Novo Airão. The DOM fingerprints of other extensive WSE systems in the upper Rio Negro basin remain to be revealed but emerge as a likely source (Adeney et al., 2016; Ríos-Villamizar et al., 2020). Besides more Rio Negro baseline DOM data, flooded forests (igapós) must be included as potential sources of DOM markers as well to study their difference from more elevated valley and upland WSE's.

PubChem suggested naphthalene or chromene structures for smaller molecules (<15 C atoms, $mz < 300$) that are oxygen-poor scaffolds consisting of two rings. Larger molecules suggestions were dominated by ring structures with a higher degree of oxidation and functionalization. PubChem suggestions represent only a first indication of potential structures and not necessarily structures that were identified in DOM or organisms. Phenols chromenes and benzofurans are well known photo- and bioactive plant metabolites (Towers and Hudson, 1987) and more efforts are required to identify soluble plant metabolites in tropical forests and soils. Tailored chromatographic techniques (LC-MS) are needed for the targeted analysis of these biological relevant ecosystem markers in future (Petras et al., 2017).

4.5. Implications of molecular ecosystem links for models of watersheds and river basins

Groundwater SPE-DOM markers revealed a potential direct link between ecosystem-specific headwater and ecosystem-integrated downstream signals in the Rio Negro basin. The consistent overlap of upland whitesand ecosystems and Rio Negro markers was unexpected because our initial hypothesis – a dominant riparian valley source – had to be refused. Oxidized, aromatic upland WSE markers represent a potential molecular link between headwaters and the Rio Negro. Hydromorphic soils are thought to cover more than 40% of the region under study (Junk, 1993), and have been assumed as a main source of DOC markers in blackwater watersheds (Meyer and Edwards, 1990; Dosskey and Bertsch, 1994; Hedges et al., 1994; McClain et al., 1997; Remington et al., 2007; Bardy et al., 2011; Abril et al., 2014) but their missing unique downstream molecular imprint provides evidence for the importance of upland ecosystems in control of downstream indicative DOM characteristics within the land-to-ocean continuum. While riparian valley corridors likely contribute the major part of the annual DOC export due to constant water supply from adjacent plateaus and their wider spatial distribution in the region (Remington et al., 2007; Miguez-Macho and Fan, 2012a; Miguez-Macho and Fan, 2012b), they may contribute markers to the DOM pool that do not allow to discern watersheds chemically. Our results suggest that transport-limited DOC export models (Musolff et al., 2017; Zarnetske et al., 2018) may not be appropriate to explain molecular characteristics of the exported SPE-DOC (Pereira et al., 2014; Wagner et al., 2019), but these

first results require further study including seasonal variation, for example. We find that small watersheds with strong terrestrial-lotic linkages can leave a distinct imprint within the watershed's exported DOM, although contributing only secondarily to the overall area, fluxes of water, and maybe, DOC (compare e.g., Ågren et al., 2007). For example, the smaller upland WSE watershed shows a two times lower average annual stream discharge per area but a two–three times higher annual DOC export (Supporting Information Text S1; Monteiro et al., 2014; Zanchi et al., 2015).

We diagnosed potential links between downstream and headwater SPE-DOM and present markers that potentially allow for qualitative ecosystem recognition further downstream. These markers may serve as new proxies of land-derived primary production in the Rio Negro basin if properly calibrated. For their future application it will be essential to better understand a) why these markers escape (degradability, contact time with soil, recalcitrance) and b) if they behave conservative in the land-to-ocean continuum (Hedges et al., 1994; Hutchins et al., 2017; Simon et al., 2019; Richey et al., 2021). Several authors have noted delayed oxidation and low photodegradation rates of DOM in blackwater streams (Meyer and Edwards, 1990; Remington et al., 2011; Amaral et al., 2013) which may be explained by a unique combination of low availability of nutrients, high acidity, and DOM quality (degradability, self-shading, etc., Goulding et al., 1988), and may thus constitute the molecular links described herein.

In general, our results indicate that stream samples are a suitable proxy of groundwater molecular composition in headwater catchments (Fig. 3). In contrast, the molecular composition of Rio Negro SPE-DOM (Gonsior et al., 2016; Simon et al., 2019) was 1) more homogenous than in groundwaters, and 2) largely different from groundwaters as well as 3) headwater streams (Supporting Information Figure S12). Therefore, drastic molecular changes can be expected during downstream transit (Hutchins et al., 2017). In line with this, only one of the nine most robust WSE markers in Rio Negro DOM ($C_{10}H_{12}O_7$) was part of a well-constrained set of 184 terrestrial river DOM markers (Medeiros et al., 2016), and four ($C_{10}H_{12}O_7$, $C_{21}H_{12}O_8$, $C_{22}H_{14}O_9$, $C_{20}H_{14}O_{11}$) were found to be photo-labile in a set of 2770 Congo river DOM formulae (Stubbins et al., 2010). None was found however in sets of 238 specific Lena river markers (Dubinenkov et al., 2015) or 76 Yenisej river markers (Roth et al., 2014). Based on all 239 potential Rio Negro markers from the upland WSE (114 from Simon et al., 2019, 119 from Gonsior et al. 2016, and six shared, Fig. 5), 6% were part of the terrestrial river DOM signature (Medeiros et al., 2016), 55% were also found in Congo DOM and entirely classified as photo-labile (Stubbins et al., 2010; and including the 6% of general terrestrial river markers), but overlap with boreal river markers remained low (5% in Lena, 0.4% in Yenisej; Roth et al., 2014; Dubinenkov et al., 2015). Given the available data, two similarly large fractions of upland WSE markers can thus be regarded as being specific to tropical rivers or the Rio Negro catchment. However, looking at soil DOM, five out of the nine most robust WSE markers ($C_{11}H_6O_6$, $C_{11}H_6O_8$, $C_{12}H_{10}O_7$, $C_{17}H_8O_7$,

$C_{20}H_{14}O_{11}$) and 30% of all potential upland Rio Negro markers were also correlated with low pH and high DOC in temperate forest soils (Roth et al., 2015). This means that these markers are not exclusively specific to acidic tropical forests but may be indicative of acidic systems in general. The relatively small overlap with river markers, especially constrained ones (Medeiros et al., 2016), calls for dedicated studies of markers of "retentive ecosystems" (low permeability of rocks/ soils), for example in the framework of the regional chromatography model (Hedges et al., 1994) or other models that include measures of catchment "complexity" (Jehn et al., 2021; Werner et al., 2021). Their DOM signature may be masked by large amounts of photolabile, ^{14}C-young markers from less retentive ecosystems but could be important for DOM source annotation on larger spatial scales (Pereira et al., 2014; Cao et al., 2018; Kellerman et al., 2018; Dean et al., 2019).

Relatively large overlap with acidic soil and tropical river DOM, and low recoveries of DOM by SPE thus limit the direct transferability of results to estimates of DOC export or unambiguous ecosystem identification. Although SPE-DOM properties and earlier reports of DOM aligned well (Supporting Information Figure S13), SPE only recovered 71% of WSE-DOM and 23% of plateau DOM (on average) which leaves substantial amounts of hydrophilic, neutral or biopolymeric compounds uncharacterized (Raeke et al., 2016; Patriarca et al., 2020). However, to begin revealing trends across DOM datasets, further comparative studies as the one presented here are needed to diagnose molecular links across the land-to-ocean continuum. Along with that, and to properly interpret these links, stability of markers and systematic bias in their detection due to DOM isolation or ionization needs to be further evaluated (Li et al., 2016; Hawkes et al., 2020; Patriarca et al., 2020).

5. CONCLUSION

New sets of markers are needed to better constrain variations in land-derived DOM exports and losses within aquatic systems, especially in the tropics, which account for 62 – 66 % of riverine DOC exports. We provide molecular evidence of long-assumed hypothetical links drawn from the simultaneous occurrence of tropical whitesand ecosystems (WSEs) and blackwater rivers at the example of the Rio Negro basin (Goulding et al., 1988, and references therein), which represents the largest blackwater river basin globally. Against initial expectation, we found little indication that large valley WSEs contribute soluble DOM markers that allow to distinguish the Rio Negro from other Amazon basin rivers but identified upland WSEs as their potential source. The twofold larger annual discharge and hundred-fold larger size of the valley watershed seemingly do not result in the transfer of DOM markers downstream, as expected from transport-limited DOC leaching. This discrepancy stresses the importance of specific ecosystems for DOM information content at higher-order stages of the aquatic continuum, and how it may inform hydrological models that include qualitative DOC data. The molecular composition of SPE-DOM at different stages of the aquatic

continuum emerges as a qualitative measure of DOM exports that complements quantitative DOC data. The interconnected nature and multivariate complexity of DOM shows high potential to allow studying multiple source contributions and processes simultaneously. Knowledge of the spatial distribution of aquifer and soil permeabilities and dynamics of flow paths need to be integrated with quantity (DOC) and quality (molecular composition) of headwater DOM exports. Further studies of marker stability in the land-to-ocean continuum and bias during isolation and ionization for FT-MS analysis are also warranted to correctly interpret diagnostic molecular links. Finally, consequent reporting and archiving of indicative sets of DOM markers, and intercomparisons between labs and datasets from different stages of the land-to-ocean continuum will be key to identify robust markers of ecosystem- and watershed-resolved terrestrial DOM exports.

6. RESEARCH DATA

Research Data associated with this article can be accessed at PANGAEA - Data Publisher for Earth & Environmental Science online and free of charge via the DOI: https://doi.pangaea.de/10.1594/PANGAEA.922606.

Declaration of Competing Interest

The authors declare that the research was conducted in the absence of any commercial or financial relationships that could be construed as a potential conflict of interest.

APPENDIX A. SUPPLEMENTARY MATERIAL

Supplementary data to this article can be found online at https://doi.org/10.1016/j.gca.2021.06.036.

REFERENCES

Abbott B. W., Gruau G., Zarnetske J. P., Moatar F., Barbe L., Thomas Z., Fovet O., Kolbe T., Gu S., Pierson-Wickmann A. C., Davy P. and Pinay G. (2018) Unexpected spatial stability of water chemistry in headwater stream networks. *Ecol. Lett.* **21**, 296–308.

Abril G., Martinez J.-M., Artigas L. F., Moreira-Turcq P., Benedetti M. F., Vidal L., Meziane T., Kim J.-H., Bernardes M. C., Savoye N., Deborde J., Souza E. L., Albéric P., Landim de Souza M. F. and Roland F. (2014) Amazon River carbon dioxide outgassing fuelled by wetlands. *Nature* **505**, 395–398.

Adeney J. M., Christensen N. L., Vicentini A. and Cohn-Haft M. (2016) White-sand ecosystems in Amazonia. *Biotropica* **48**, 7–23.

Ågren A., Buffam I., Jansson M. and Laudon H. (2007) Importance of seasonality and small streams for the landscape regulation of dissolved organic carbon export. *J. Geophys. Res. Biogeosci.* **112**, 1–11.

Alvarez-Cobelas M., Angeler D. G., Sánchez-Carrillo S. and Almendros G. (2012) A worldwide view of organic carbon export from catchments. *Biogeochemistry* **107**, 275–293.

Amaral J. H. F., Suhett A. L., Melo S. and Farjalla V. F. (2013) Seasonal variation and interaction of photodegradation and microbial metabolism of DOC in black water Amazonian ecosystems. *Aquat. Microb. Ecol.* **70**, 157–168.

Bardy M., Derenne S., Allard T., Benedetti M. F. and Fritsch E. (2011) Podzolisation and exportation of organic matter in black waters of the Rio Negro (upper Amazon basin, Brazil). *Biogeochemistry* **106**, 71–88.

Benk S. A., Li Y., Roth V.-N. and Gleixner G. (2018) Lignin Dimers as Potential Markers for 14C-young Terrestrial Dissolved Organic Matter in the Critical Zone. *Front. Earth Sci.*, 1–9.

Bernhardt E. S., Heffernan J. B., Grimm N. B., Stanley E. H., Harvey J. W., Arroita M., Appling A. P., Cohen M. J., McDowell W. H., Hall R. O., Read J. S., Roberts B. J., Stets E. G. and Yackulic C. B. (2018) The metabolic regimes of flowing waters. *Limnol. Oceanogr.* **63**, 99–118.

Bhattacharyya A., Campbell A. N., Tfaily M. M., Lin Y., Kukkadapu R. K., Silver W. L., Nico P. S. and Pett-Ridge J. (2018) Redox Fluctuations Control the Coupled Cycling of Iron and Carbon in Tropical Forest Soils. *Environ. Sci. Technol.* **52**, 14129–14139.

Bowen G. J. and Revenaugh J. (2003) Interpolating the isotopic composition of modern meteoric precipitation. *Water Resour. Res.* **39**, 1–13.

Boye K., Noël V., Tfaily M. M., Bone S. E., Williams K. H., Bargar J. R. and Fendorf S. (2017) Thermodynamically controlled preservation of organic carbon in floodplains. *Nat. Geosci.* **10**, 415–419.

Cao X., Aiken G. R., Butler K. D., Huntington T. G., Balch W. M., Mao J. and Schmidt-Rohr K. (2018) Evidence for major input of riverine organic matter into the ocean. *Org. Geochem.* **116**, 62–76.

Chassé A. W., Ohno T., Higgins S. R., Amirbahman A., Yildirim N. and Parr T. B. (2015) Chemical force spectroscopy evidence supporting the layer-by-layer model of organic matter binding to iron (oxy)hydroxide mineral surfaces. *Environ. Sci. Technol.* **49**, 9733–9741.

Coynel A., Seyler P., Etcheber H., Meybeck M. and Orange D. (2005) Spatial and seasonal dynamics of total suspended sediment and organic carbon species in the Congo River. *Global Biogeochem. Cycles* **19**, 1–17.

Creed I. F., McKnight D. M., Pellerin B. A., Green M. B., Bergamaschi B. A., Aiken G. R., Burns D. A., Findlay S. E. G.,

Shanley H., Striegl R. G., Aulenbach B. T., Clow D. W., Laudon H., McGlynn B. L., McGuire K. J., Smith R. A. and Stackpoole S. M. (2015) The river as a chemostat: fresh perspectives on dissolved organic matter flowing down the river continuum. *Can. J. Fish. Aquat. Sci.* **72**, 1272–1285.

Dai M., Yin Z., Meng F., Liu Q. and Cai W.-J. (2012) Spatial distribution of riverine DOC inputs to the ocean: An updated global synthesis. *Curr. Opin. Environ. Sustain.* **4**, 170–178.

Dean J. F., Garnett M. H., Spyrakos E. and Billett M. F. (2019) The potential hidden age of dissolved organic carbon exported by peatland streams. *J. Geophys. Res. Biogeosciences* **124**, 328–341.

Demarchi L. O., Scudeller V. V., Moura L. C., Dias-Terceiro R. G., Lopes A., Wittmann F. K. and Piedade M. T. F. (2018) Floristic composition, structure and soil-vegetation relations in three white-sand soil patches in central Amazonia. *Acta Amaz.* **48**, 46–56.

Dittmar T., Koch B., Hertkorn N. and Kattner G. (2008) A simple and efficient method for the solid-phase extraction of dissolved organic matter (SPE-DOM) from seawater. *Limnol. Oceanogr. Methods* **6**, 230–235.

Dosskey M. G. and Bertsch P. M. (1994) Forest sources and pathways of organic matter transport to a blackwater stream : A hydrologic approach. *Biogeochemistry* **24**, 1–19.

Drake T. W., Guillemette F., Hemingway J. D., Chanton J. P., Podgorski D. C., Zimov N. S. and Spencer R. G. M. (2018a) The ephemeral signature of permafrost Carbon in an Arctic fluvial network. *J. Geophys. Res. Biogeosciences* **123**, 1475–1485.

Drake T. W., Van Oost K., Barthel M., Bauters M., Hoyt A. M., Podgorski D. C., Six J., Boeckx P., Trumbore S. E., Cizungu Ntaboba L. and Spencer R. G. M. (2019) Mobilization of aged and biolabile soil carbon by tropical deforestation. *Nat. Geosci.* **12**, 541–546.

Drake T. W., Raymond P. A. and Spencer R. G. M. (2018b) Terrestrial carbon inputs to inland waters: A current synthesis of estimates and uncertainty. *Limnol. Oceanogr. Lett.* **3**, 132–142.

Dubinenkov I., Flerus R., Schmitt-Kopplin P., Kattner G. and Koch B. P. (2015) Origin-specific molecular signatures of dissolved organic matter in the Lena Delta. *Biogeochemistry* **123**, 1–14.

Ertel J. R., Hedges J. I., Devol A. H., Richey J. E. and De Nazare Goes Ribeiro E. (1986) Dissolved humic substances of the Amazon River system. *Limnol. Oceanogr.* **31**, 739–754.

Gehre M., Geilmann H., Richter J., Werner R. A. and Brand W. A. (2004) Continuous flow 2H/1H and 18O/ 16O analysis of water samples with dual inlet precision. *Rapid Commun. Mass Spectrom.* **18**, 2650–2660.

Gleixner G., Poirier N., Bol R. and Balesdent J. (2002) Molecular dynamics of organic matter in a cultivated soil. *Org. Geochem.* **33**, 357–366.

Gonsior M., Valle J., Schmitt-Kopplin P., Hertkorn N., Bastviken D., Luek J., Harir M., Bastos W. and Enrich-Prast A. (2016) Chemodiversity of dissolved organic matter in the Amazon Basin. *Biogeosciences* **13**, 4279–4290.

Goulding M., Carvalho M. L. and Ferreira E. G. (1988). In *Blackwaters. In Rio Negro, rich life in poor water. Amazonian diversity and foodchain ecology as seen through fish communities*. Academic Publishing, The Hague, pp. 29–36.

Graven H. D. (2015) Impact of fossil fuel emissions on atmospheric radiocarbon and various applications of radiocarbon over this century. *Proc. Natl. Acad. Sci.* **112**, 9542–9545.

Guinoiseau D., Bouchez J., Gélabert A., Louvat P., Filizola N. and Benedetti M. F. (2016) The geochemical filter of large river confluences. *Chem. Geol.* **441**, 191–203.

Hawkes J. A., D'Andrilli J., Agar J. N., Barrow M. P., Berg S. M., Catalán N., Chen H., Chu R. K., Cole R. B., Dittmar T., Gavard R., Gleixner G., Hatcher P. G., He C., Hess N. J., Hutchins R. H. S., Ijaz A., Jones H. E., Kew W., Khaksari M., Lozano D. C. P., Lv J., Mazzoleni L., Noriega-Ortega B., Osterholz H., Radoman N., Remucal C. K., Schmitt N. D., Schum S., Shi Q., Simon C., Singer G., Sleighter R. S., Stubbins A., Thomas M. J., Tolic N., Zhang S., Zito P. and Podgorski D. C. (2020) An international laboratory comparison of dissolved organic matter composition by high resolution mass spectrometry: Are we getting the same answer? *Limnol. Oceanogr. Methods* **18**, 235–258.

Hawkes J. A., Dittmar T., Patriarca C., Tranvik L. and Bergquist J. (2016) Evaluation of the Orbitrap Mass Spectrometer for the Molecular Fingerprinting Analysis of Natural Dissolved Organic Matter. *Anal. Chem.* **88**, 7698–7704.

Hedges J. I., Clark W. A., Quay P. D., Richey J. E., Devol A. H. and Santos U. de M. (1986a) Compositions and fluxes of particulate organic material in the Amazon River. *Limnol. Oceanogr.* **31**, 717–738.

Hedges J. I., Cowie G. L., Richey J. E., Quay P. D., Benner R., Strom M. and Forsberg B. R. (1994) Origins and processing of organic matter in the Amazon River as indicated by carbohydrates and amino acids. *Limnol. Oceanogr.* **39**, 743–761.

Hedges J. I., Ertel J. R., Quay P. D., Grootes P. M., Richey J. E., Devol A. H., Farwell G. W., Schmidt F. W. and Salati E. (1986b) Organic Carbon-14 in the Amazon River system. *Science (80-.)* **231**, 1129–1131.

Hernes P. J., Robinson A. C. and Aufdenkampe A. K. (2007) Fractionation of lignin during leaching and sorption and implications for organic matter "freshness". *Geophys. Res. Lett.* **34**, 1–6.

Hertkorn N., Harir M., Koch B. P., Michalke B. and Schmitt-Kopplin P. (2013) High-field NMR spectroscopy and FTICR mass spectrometry: Powerful discovery tools for the molecular level characterization of marine dissolved organic matter. *Biogeosciences* **10**, 1583–1624.

Herzsprung P., Hertkorn N., von Tümpling W., Harir M., Friese K. and Schmitt-Kopplin P. (2014) Understanding molecular formula assignment of Fourier transform ion cyclotron resonance mass spectrometry data of natural organic matter from a chemical point of view. *Anal. Bioanal. Chem.* **406**, 7977–7987.

Huang T. H., Fu Y. H., Pan P. Y. and Chen C. T. A. (2012) Fluvial carbon fluxes in tropical rivers. *Curr. Opin. Environ. Sustain.* **4**, 162–169.

Hutchins R. H. S., Aukes P., Schiff S. L., Dittmar T., Prairie Y. T. and del Giorgio P. A. (2017) The Optical, Chemical, and Molecular Dissolved Organic Matter Succession Along a Boreal Soil-Stream-River Continuum. *J. Geophys. Res. Biogeosciences* **122**, 2892–2908.

James J. N., Gross C. D., Dwivedi P., Myers T., Santos F., Bernardi R., Fidalgo de Faria M., Amaral Guerrini I., Harrison R. and Butman D. (2019) Land use change alters the radiocarbon age and composition of soil and water-soluble organic matter in the Brazilian Cerrado. *Geoderma* **345**, 38–50.

Janzen D. H. (1974) Tropical blackwater rivers, animals, and mast fruiting by the Dipterocarpaceae. *Biotropica* **6**, 69–103.

Jasechko S. and Taylor R. G. (2015) Intensive rainfall recharges tropical groundwaters. *Environ. Res. Lett.* **10** 124015.

Jehn F. U., Bestian K., Breuer L., Kraft P. and Houska T. (2020) Using hydrological and climatic catchment clusters to explore drivers of catchment behavior. *Hydrol. Earth Syst. Sci.* **24**, 1081–1100.

Jehn F. U., Breuer L., Kraft P., Bestian K. and Houska T. (2021) Simple Catchments and Where to Find Them: The Storage-

Discharge Relationship as a Proxy for Catchment Complexity. *Front. Water* **3** 631651.

Junk W. J. (1993) Wetlands of tropical South America. In *Wetlands of the world: Inventory, ecology and management* (eds. D. F. Whigham, D. Dykyjová and S. Hejný). Springer Science +Business Media B.V, Heidelberg, pp. 679–739.

Junk W. J., Piedade M. T. F., Schöngart J., Cohn-Haft M., Adeney J. M. and Wittmann F. (2011) A classification of major naturally-occurring Amazonian Lowland Wetlands. *Wetlands* **31**, 623–640.

Kellerman A. M., Guillemette F., Podgorski D. C., Aiken G. R., Butler K. D. and Spencer R. G. M. (2018) Unifying concepts linking dissolved organic matter composition to persistence in aquatic ecosystems. *Environ. Sci. Technol.* **52**, 2538–2548.

Klinge H. and Medina E. (1978) Rio Negro caatingas and campinas, Amazonas States of Venezuela and Brazil. In Ecosystems of the World: Heathlands and related shrublands. Ecosystems of the World. *A. Descriptive studies (ed. R. L. Specht). Elsevier, Amsterdam*, 483–488.

Kunert N., Aparecido L. M. T., Wolff S., Higuchi N., Dos Santos J., De Araujo A. C. and Trumbore S. (2017) A revised hydrological model for the Central Amazon: The importance of emergent canopy trees in the forest water budget. *Agric. For. Meteorol.* **239**, 47–57.

Laudon H. and Sponseller R. A. (2018) How landscape organization and scale shape catchment hydrology and biogeochemistry: insights from a long-term catchment study. *Wiley Interdiscip. Rev. Water* **5** e1265.

Ledesma J. L. J., Grabs T., Bishop K. H., Schiff S. L. and Köhler S. J. (2015) Potential for long-term transfer of dissolved organic carbon from riparian zones to streams in boreal catchments. *Glob. Chang. Biol.* **21**, 2963–2979.

Leenheer J. A. (1980) Origin and nature of humic substances in the waters of the Amazon River Basin. *Acta Amaz.* **10**, 513–526.

Leopoldo P. R., Matsui E., Salati E., Franken W. and Ribeiro M. de N. G. (1982) Composição isotópica da água de chuva e da água do solo em floresta amazônica do tipo terra firme, região de Manaus. *Acta Amaz.* **12**, 7–13.

Li M., Peng C., Zhou X., Yang Y., Guo Y., Shi G. and Zhu Q. (2019) Modeling global riverine DOC flux dynamics from 1951 to 2015. *J. Adv. Model. Earth Syst.* **11**, 514–530.

Li Y., Harir M., Lucio M., Kanawati B., Smirnov K., Flerus R., Koch B. P., Schmitt-Kopplin P. and Hertkorn N. (2016) Proposed Guidelines for Solid Phase Extraction of Suwannee River Dissolved Organic Matter. *Anal. Chem.* **88**, 6680–6688.

Lucas Y., Montes C. R., Mounier S., Loustau Cazalet M., Ishida D., Achard R., Garnier C., Coulomb B. and Melfi A. J. (2012) Biogeochemistry of an Amazonian podzol-ferralsol soil system with white kaolin. *Biogeosciences* **9**, 3705–3720.

Luizão R. C. C., Luizão F. J., Paiva R. Q., Monteiro T. F., Sousa L. S. and Kruijt B. (2004) Variation of carbon and nitrogen cycling processes along a topographic gradient in a central Amazonian forest. *Glob. Chang. Biol.* **10**, 592–600.

Lv S., Yu Q., Wang F., Wang Y., Yan W. and Li Y. (2019) A synthetic model to quantify dissolved organic carbon transport in the Changjiang River system: Model structure and spatiotemporal patterns. *J. Adv. Model. Earth Syst.* **11**, 3024–3041.

Lynch L. M., Sutfin N. A., Fegel T. S., Boot C. M., Covino T. P. and Wallenstein M. D. (2019) River channel connectivity shifts metabolite composition and dissolved organic matter chemistry. *Nat. Commun.* **10**, 459.

Marques J. D. de O., Libardi P. L., Teixeira W. G. and Reis A. M. (2004) Estudo de parâmetros físicos, químicos e hídricos de um Latossolo Amarelo, na região Amazônica. *Acta Amaz.* **34**, 145–154.

Marques de O. J. D., Luizão F. J., Teixeira W. G., Vitel C. M. and Marques de A. E. M. (2016) Soil organic carbon, carbon stock and their relationships to physical attributes under forest soils in central Amazonia. *Rev. Árvore* **40**, 197–208.

Marques J. D. de O., Teixeira W. G., Reis A. M., Cruz Junior O. F., Batista S. M. and Afonso M. A. C. B. (2010) Atributos químicos, físico-hídricos e mineralogia da fração argila em solos do Baixo Amazonas: Serra de Parintins. *Acta Amaz.* **40**, 01–12.

Marschner B., Brodowski S., Dreves A., Gleixner G., Gude A., Grootes P. M., Hamer U., Heim A., Jandl G., Ji R., Kaiser K., Kalbitz K., Kramer C., Leinweber P., Rethemeyer J., Schäffer A., Schmidt M. W. I., Schwark L. and Wiesenberg G. L. B. (2008) How relevant is recalcitrance for the stabilization of organic matter in soils? *J. Plant Nutr. Soil Sci.* **171**, 91–110.

Mayorga E., Aufdenkampe A. K., Masiello C. A., Krusche A. V., Hedges J. I., Quay P. D., Richey J. E. and Brown T. A. (2005) Young organic matter as a source of carbon dioxide outgassing from Amazonian rivers. *Nature* **436**, 538–541.

McClain M. E., Richey J. E., Brandes J. A. and Pimentel T. P. (1997) Dissolved organic matter and terrestrial-lotic linkages in the central Amazon basin of Brazil. *Global Biogeochem. Cycles* **11**, 295–311.

McClain M. E., Richey J. E. and Pimentel T. P. (1994) Ground-water nitrogen dynamics at the terrestrial-lotic interface of a small catchment in the Central Amazon basin. *Biogeochemistry* **27**, 113–127.

McGuire K. J., Torgersen C. E., Likens G. E., Buso D. C., Lowe W. H. and Bailey S. W. (2014) Network analysis reveals multiscale controls on streamwater chemistry. *Proc. Natl. Acad. Sci. USA* **111**, 7030–7035.

Medeiros P. M., Seidel M., Niggemann J., Spencer R. G. M., Hernes P. J., Yager P. L., Miller W. L., Dittmar T. and Hansell D. A. (2016) A novel molecular approach for tracing terrigenous dissolved organic matter into the deep ocean. *Global Biogeochem. Cycles* **30**, 1–11.

Melack J. M. and Hess L. L. (2010) Remote Sensing of the Distribution and Extent of Wetlands in the Amazon Basin. In Amazonian Floodplain Forests: Ecophysiology, Biodiversity and Sustainable Management. Ecological Studies 210 (eds. W. J. Junk, M. T. F. Piedade, F. Wittmann, J. Schöngart, and P. Parolin). Springer Science+Business Media B.V., Heidelberg. pp. 43–59.

Meyer J. L. and Edwards R. T. (1990) Ecosystem metabolism and turnover of organic carbon along a blackwater river continuum. *Ecology* **71**, 668–677.

Miguez-Macho G. and Fan Y. (2012a) The role of groundwater in the Amazon water cycle: 1. Influence on seasonal streamflow, flooding and wetlands. *J. Geophys. Res. Atmos.* **117**, D15113.

Miguez-Macho G. and Fan Y. (2012b) The role of groundwater in the Amazon water cycle: 2. Influence on seasonal soil moisture and evapotranspiration. *J. Geophys. Res. Atmos.* **117**, D15114.

Monteiro M. T. F., Oliveira S. M., Luizão F. J., Cândido L. A., Ishida F. Y. and Tomasella J. (2014) Dissolved organic carbon concentration and its relationship to electrical conductivity in the waters of a stream in a forested Amazonian blackwater catchment. *Plant Ecol. Divers.* **7**, 205–213.

Montes C. R., Lucas Y., Pereira O. J. R., Achard R., Grimaldi M. and Melfi A. J. (2011) Deep plant-derived carbon storage in Amazonian podzols. *Biogeosciences* **8**, 113–120.

Moore S., Evans C. D., Page S. E., Garnett M. H., Jones T. G., Freeman C., Hooijer A., Wiltshire A. J., Limin S. H. and Gauci V. (2013) Deep instability of deforested tropical peatlands revealed by fluvial organic carbon fluxes. *Nature* **493**, 660–663.

Musolff A., Fleckenstein J. H., Rao P. S. C. and Jawitz J. W. (2017) Emergent archetype patterns of coupled hydrologic and

biogeochemical responses in catchments. *Geophys. Res. Lett.* **44**, 4143–4151.

Do Nascimento N. R., Bueno G. T., Fritsch E., Herbillon A. J., Allard T., Melfi A. J., Astolfo R., Boucher H. and Li Y. (2004) Podzolization as a deferralitization process: a study of an Acrisol-Podzol sequence derived from Palaeozoic sandstones in the northern upper Amazon Basin. *Eur. J. Soil Sci.* **55**, 523–538.

Do Nascimento N. R., Fritsch E., Bueno G. T., Bardy M., Grimaldi C. and Melfi A. J. (2008) Podzolization as a deferralitization process: Dynamics and chemistry of ground and surface waters in an Acrisol - Podzol sequence of the upper Amazon Basin. *Eur. J. Soil Sci.* **59**, 911–924.

Newcomb C. J., Qafoku N. P., Grate J. W., Bailey V. L. and De Yoreo J. J. (2017) Developing a molecular picture of soil organic matter-mineral interactions by quantifying organo-mineral binding. *Nat. Commun.* **8**, 396.

Oksanen J. (2010) Multivariate analysis of ecological communities in R: vegan tutorial. , 43. Available at: cc.oulu.fi/~jarioksa/opetus/metodi/vegantutor.pdf [Accessed April 6, 2015].

Osterholz H., Singer G., Wemheuer B., Daniel R., Simon M., Niggemann J. and Dittmar T. (2016) Deciphering associations between dissolved organic molecules and bacterial communities in a pelagic marine system. *ISME J.* **10**, 1717–1730.

Patriarca C., Balderrama A., Može M., Sjöberg P. J. R., Bergquist J., Tranvik L. J. and Hawkes J. A. (2020) Investigating the Ionization of Dissolved Organic Matter by Electrospray. *Anal. Chem.* **92**, 14210–14218.

Pereira R., Bovolo C. I., Spencer R. G. M., Hernes P. J., Tipping E., Vieth-Hillebrand A., Pedentchouk N., Chappell N. A., Parkin G. and Wagner T. (2014) Mobilization of optically invisible dissolved organic matter in response to rainstorm events in a tropical forest headwater river. *Geophys. Res. Lett.* **41**, 1202–1208.

Petras D., Koester I., Da Silva R., Stephens B. M., Haas A. F., Nelson C. E., Kelly L. W., Aluwihare L. I. and Dorrestein P. C. (2017) High-resolution liquid chromatography tandem mass spectrometry enables large scale molecular characterization of dissolved organic matter. *Front. Mar. Sci.* **4**, 406.

Powers L. C., Hertkorn N., McDonald N., Schmitt-Kopplin P., Del Vecchio R., Blough N. V. and Gonsior M. (2019) Sargassum sp. act as a large regional source of marine dissolved organic carbon and polyphenols. *Global Biogeochem. Cycles* **33**, 1423–1439.

Quay P. D., Wilbur D. O., Richey J. E., Hedges J. I., Devol A. H. and Victoria R. (1992) Carbon cycling in the Amazon River: Implications from the 13C compositions of particles and solutes. *Limnol. Oceanogr.* **37**, 857–871.

Quesada C. A., Lloyd J., Anderson L. O., Fyllas N. M., Schwarz M. and Czimczik C. I. (2011) Soils of Amazonia with particular reference to the RAINFOR sites. *Biogeosciences* **8**, 1415–1440.

Raeke J., Lechtenfeld O. J., Tittel J., Oosterwoud M. R., Bornmann K. and Reemtsma T. (2017) Linking the mobilization of dissolved organic matter in catchments and its removal in drinking water treatment to its molecular characteristics. *Water Res.* **113**, 149–159.

Raeke J., Lechtenfeld O. J., Wagner M., Herzsprung P. and Reemtsma T. (2016) Selectivity of solid phase extraction of freshwater dissolved organic matter and its effect on ultrahigh resolution mass spectra. *Environ. Sci. Process. Impacts* **18**, 918–927.

Raymond P. A. and Spencer R. G. M. (2014) Riverine DOM. In *Biogeochemistry of Marine Dissolved Organic Matter* (eds. D. A. Hansell and C. A. Carlson), Second Edition. Academic Press, Cambridge, pp. 509–533.

Regnier P., Friedlingstein P., Ciais P., Mackenzie F. T., Gruber N., Janssens I. A., Laruelle G. G., Lauerwald R., Luyssaert S.,

Andersson A., Arndt S., Arnosti C., Borges A. V., Dale A. W., Gallego-Sala A., Goddéris Y., Goossens N., Hartmann J., Heinze C., Ilyina T., Joos F., Larowe D. E., Leifeld J., Meysman F. J. R., Munhoven G., Raymond P. A., Spahni R., Suntharalingam P. and Thullner M. (2013) Anthropogenic perturbation of the carbon fluxes from land to ocean. *Nat. Geosci.* **6**, 597–607.

Remington S., Krusche A. and Richey J. (2011) Effects of DOM photochemistry on bacterial metabolism and CO2 evasion during falling water in a humic and a whitewater river in the Brazilian Amazon. *Biogeochemistry* **105**, 185–200.

Remington S. M., Strahm B. D., Neu V., Richey J. E. and Da Cunha H. B. (2007) The role of sorption in control of riverine dissolved organic carbon concentrations by riparian zone soils in the Amazon basin. *Soil Sci.* **172**, 279–291.

Richey J. E., Spencer R. G. M., Ward N. D. and Drake T. W. (2021) Fluvial Carbon Dynamics across the Land to Ocean Continuum of Great Tropical Rivers: the Amazon and Congo. *Earth Sp. Sci. Open Arch.*, 1–53.

Riedel T. and Dittmar T. (2014) A Method Detection Limit for the Analysis of Natural Organic Matter via Fourier Transform Ion Cyclotron Resonance Mass Spectrometry. *Anal. Chem.* **86**, 8376–8382.

Riedel T., Zark M., Vähätalo A. V., Niggemann J., Spencer R. G. M., Hernes P. J. and Dittmar T. (2016) Molecular Signatures of Biogeochemical Transformations in Dissolved Organic Matter from Ten World Rivers. *Front. Earth Sci.* **4**, 85.

Ríos-Villamizar E. A., Adeney J. M., Piedade M. T. F. and Junk W. J. (2020) New insights on the classification of major Amazonian river water types. *Sustain. Water Resour. Manag.* **6**, 83.

Roth V.-N., Dittmar T., Gaupp R. and Gleixner G. (2014) Ecosystem-specific composition of dissolved organic matter. *Vadose Zo. J.* **13**.

Roth V.-N., Dittmar T., Gaupp R. and Gleixner G. (2015) The Molecular Composition of Dissolved Organic Matter in Forest Soils as a Function of pH and Temperature. *PLoS One* **10** e0119188.

Roth V.-N., Lange M., Simon C., Hertkorn N., Bucher S., Goodall T., Griffiths R. I., Mellado-Vázquez P. G., Mommer L., Oram N. J., Weigelt A., Dittmar T. and Gleixner G. (2019) Persistence of dissolved organic matter explained by molecular changes during its passage through soil. *Nat. Geosci.* **12**, 755–761.

Rousk J., Bååth E., Brookes P. C., Lauber C. L., Lozupone C., Caporaso J. G., Knight R. and Fierer N. (2010) Soil bacterial and fungal communities across a pH gradient in an arable soil. *ISME J.* **4**, 1340–1351.

Seyler F., Muller F., Cochonneau G., Guimarães L. and Guyot J. L. (2009) Watershed delineation for the Amazon sub-basin system using GTOPO30 DEM and a drainage network extracted from JERS SAR images. *Hydrol. Process.* **23**, 3173–3185.

Simon C., Osterholz H., Koschinsky A. and Dittmar T. (2019) Riverine mixing at the molecular scale – An ultrahigh-resolution mass spectrometry study on dissolved organic matter and selected metals in the Amazon confluence zone (Manaus, Brazil). *Org. Geochem.* **129**, 45–62.

Simon C., Roth V.-N., Dittmar T. and Gleixner G. (2018) Molecular Signals of Heterogeneous Terrestrial Environments Identified in Dissolved Organic Matter: A Comparative Analysis of Orbitrap and Ion Cyclotron Resonance Mass Spectrometers. *Front. Earth Sci.* **6**, 1–16.

Sioli H. (1954) Gewässerchemie und Vorgänge in den Böden im Amazonasgebiet. *Naturwissenschaften* **41**, 456–457.

Spencer R. G. M., Kellerman A. M., Podgorski D. C., Macedo M. N., Jankowski K. J., Nunes D. and Neill C. (2019) Identifying the Molecular Signatures of Agricultural Expansion in Amazonian Headwater Streams. *J. Geophys. Res. Biogeosciences*, 1637–1650.

Steinhof A., Altenburg M. and Machts H. (2017) Sample preparation at the Jena 14C laboratory. *Radiocarbon* **59**, 815–830.

Stubbins A., Spencer R. G. M., Chen H., Hatcher P. G., Mopper K., Hernes P. J., Mwamba V. L., Mangangu A. M., Wabakanghanzi J. N. and Six J. (2010) Illuminated darkness: Molecular signatures of Congo River dissolved organic matter and its photochemical alteration as revealed by ultrahigh precision mass spectrometry. *Limnol. Oceanogr.* **55**, 1467–1477.

Stücheli P. E., Niggemann J. and Schubert C. J. (2018) Comparison of different solid phase extraction sorbents for the qualitative assessment of dissolved organic nitrogen in freshwater samples using FT-ICR-MS. *J. Limnol.* **77**, 400–411.

Tiegs S. D., Costello D. M., Isken M. W., Woodward G., McIntyre P. B., Gessner M. O., Chauvet E., Griffiths N. A., Flecker A. S., Acuña V., Albariño R., Allen D. C., Alonso C., Andino P., Arango C., Aroviita J., Barbosa M. V. M., Barmuta L. A., Baxter C. V., Bell T. D. C., Bellinger B., Boyero L., Brown L. E., Bruder A., Bruesewitz D. A., Burdon F. J., Callisto M., Canhoto C., Capps K. A., Castillo M. M., Clapcott J., Colas F., Colón-Gaud C., Cornut J., Crespo-Pérez V., Cross W. F., Culp J. M., Danger M., Dangles O., De Eyto E., Derry A. M., Villanueva V. D., Douglas M. M., Elosegi A., Encalada A. C., Entrekin S., Espinosa R., Ethaiya D., Ferreira V., Ferriol C., Flanagan K. M., Fleituch T., Shah J. J. F., Barbosa A. F., Friberg N., Frost P. C., Garcia E. A., Lago L. G., Soto P. E. G., Ghate S., Giling D. P., Gilmer A., Gonçalves J. F., Gonzales R. K., Graça M. A. S., Grace M., Grossart H. P., Guérold F., Gulis V., Hepp L. U., Higgins S., Hishi T., Huddart J., Hudson J., Imberger S., Iñiguez-Armijos C., Iwata T., Janetski D. J., Jennings E., Kirkwood A. E., Koning A. A., Kosten S., Kuehn K. A., Laudon H., Leavitt P. R., Da Silva A. L. L., Leroux S. J., LeRoy C. J., Lisi P. J., MacKenzie R., Marcarelli A. M., Masese F. O., McKie B. G., Medeiros A. O., Meissner K., Miliša M., Mishra S., Miyake Y., Moerke A., Mombrikotb S., Mooney R., Moulton T., Muotka T., Negishi J. N., Neres-Lima V., Nieminen M. L., Nimptsch J., Ondruch J., Paavola R., Pardo I., Patrick C. J., Peeters E. T. H. M., Pozo J., Pringle C., Prussian A., Quenta E., Quesada A., Reid B., Richardson J. S., Rigosi A., Rincón J., Rîşnoveanu G., Robinson C. T., Rodríguez-Gallego L., Royer T. V., Rusak J. A., Santamans A. C., Selmeczy G. B., Simiyu G., Skuja A., Smykla J., Sridhar K. R., Sponseller R., Stoler A., Swan C. M., Szlag D., Teixeira-De Mello F., Tonkin J. D., Uusheimo S., Veach A. M., Vilbaste S., Vought L. B. M., Wang C. P., Webster J. R., Wilson P. B., Woelfl S., Xenopoulos M. A., Yates A. G., Yoshimura C., Yule C. M., Zhang Y. X. and Zwart J. A. (2019) Global patterns and drivers of ecosystem functioning in rivers and riparian zones. *Sci. Adv.* **5**, 1–9.

Tomasella J., Hodnett M. G., Cuartas L. A., Nobre A. D., Waterloo M. J. and Oliveira S. M. (2007) The water balance of an Amazonian micro-catchment: The effect of interannual variability of rainfall on hydrological behaviour. *Hydrol. Process.* **22**, 2133–2147.

Towers G. H. N. and Hudson J. B. (1987) Potentially useful antimicrobial and antiviral phototoxins from plants. *Photochem. Photobiol.* **46**, 61–66.

Trumbore S. E., Sierra C. A. and Hicks Pries C. E. (2016) Radiocarbon nomenclature, theory, models, and interpretation: measuring age, determining cycling rates, and tracing source pools. In Climate, Radiocarbon and Change (eds. E. A. G.

Schuur, E. R. M. Druffel, and Susan E. Trumbore). Springer, Basel. pp. 45–82.

Vasco-Palacios A. M., Hernandez J., Peñuela-Mora M. C., Franco-Molano A. E. and Boekhout T. (2018) Ectomycorrhizal fungi diversity in a white sand forest in western Amazonia. *Fungal Ecol.* **31**, 9–18.

Waggoner D. C., Chen H., Willoughby A. S. and Hatcher P. G. (2015) Formation of black carbon-like and alicyclic aliphatic compounds by hydroxyl radical initiated degradation of lignin. *Org. Geochem.* **82**, 69–76.

Waggoner D. C., Wozniak A. S., Cory R. M. and Hatcher P. G. (2017) The role of reactive oxygen species in the degradation of lignin derived dissolved organic matter. *Geochim. Cosmochim. Acta* **208**, 171–184.

Wagner S., Fair J. H., Matt S., Hosen J. D., Raymond P. A., Saiers J., Shanley J. B., Dittmar T. and Stubbins A. (2019) Molecular hysteresis: Hydrologically driven changes in riverine dissolved organic matter chemistry during a storm event. *J. Geophys. Res. Biogeosciences* **124**, 759–774.

Waterloo M. J., Oliveira S. M., Drucker D. P., Nobre A. D., Cuartas L. A., Hodnett M. G., Langedijk I., Jans W. W. P., Tomasella J., Araujo A. C. d, Pimentel T. P. and Estrada J. C. M. (2006) Export of organic carbon in run-off from an Amazonian rainforest blackwater catchment. *Hydrol. Process.* **20**, 2581–2597.

Webb J. R., Santos I. R., Maher D. T. and Finlay K. (2018) The importance of aquatic carbon fluxes in net ecosystem carbon budgets: A catchment-scale review. *Ecosystems* **22**, 508–527.

Werner B. J., Lechtenfeld O. J., Musolff A., Rooij G. H., De Yang J., Werban U. and Fleckenstein J. H. (2021) Patterns and dynamics of dissolved organic carbon exports from a riparian zone of a temperate, forested catchment. *Hydrol. Earth Syst. Sci. Discuss.*, 1–27.

Zanchi F. B., Meesters A. G. C. A., Waterloo M. J., Kruijt B., Kesselmeier J., Luizão F. J. and Dolman A. J. (2014) Soil CO2 exchange in seven pristine Amazonian rain forest sites in relation to soil temperature. *Agric. For. Meteorol.* **192–193**, 96–107.

Zanchi F. B., Waterloo M. J., Dolman A. J., Groenendijk M., Kesselmeier J., Kruijt B., Bolson M. A., Luizão F. J. and Manzi A. O. (2011) Influence of drainage status on soil and water chemistry, litter decomposition and soil respiration in central Amazonian forests on sandy soils. *Rev. Ambient. e Agua* **6**, 6–29.

Zanchi F. B., Waterloo M. J., Tapia A. P., Alvarado Barrientos M. S., Bolson M. A., Luizão F. J., Manzi A. O. and Dolman A. J. (2015) Water balance, nutrient and carbon export from a heath forest catchment in central Amazonia. *Brazil. Hydrol. Process.* **29**, 3633–3648.

Zarnetske J. P., Bouda M., Abbott B. W., Saiers J. and Raymond P. A. (2018) Generality of hydrologic transport limitation of watershed organic Carbon flux across ecoregions of the United States. *Geophys. Res. Lett.* **45**, 11702–11711.

Zavarzina A. G., Lisov A. V. and Leontievsky A. A. (2018) The role of ligninolytic enzymes laccase and a versatile peroxidase of the white-rot fungus Lentinus tigrinus in biotransformation of soil humic matter: Comparative in vivo study. *J. Geophys. Res. Biogeosciences* **123**, 2727–2742.

Zhang X.-P., Yang Z.-L., Niu G.-Y. and Wang X.-Y. (2009) Stable water isotope simulation in different reservoirs of Manaus, Brazil, by Community Land Model incorporating stable isotopic effect. *Int. J. Climatol.* **29**, 619–628.

Associate editor: Thomas Wagner